



MARMARA UNIVERSITY
FACULTY OF ENGINEERING



ANALYSIS OF A SOLAR POWERED STIRLING ENGINE

ENES ÖZKARATAŞLİOĞLU , EBRAR İNAN

GRADUATION PROJECT REPORT

**Department of Mechanical Engineering
Supervisor**

Doç. Dr. Barış YILMAZ



MARMARA UNIVERSITY
FACULTY OF ENGINEERING



ANALYSIS OF A SOLAR POWERED STIRLING ENGINE

by

Enes ÖZKARATAŞLIOĞLU ,

Ebrar İNAN

June 8 , 2023 Istanbul

**SUBMITTED TO THE DEPARTMENT OF MECHANICAL ENGINEERING
IN PARTIAL FULFILLMENT OF THE REQUIREMENTS FOR THE DEGREE
OF
BACHELOR OF SCIENCE
AT
MARMARA UNIVERSITY**

The author(s) hereby grant(s) to Marmara University permission to reproduce and to distribute publicly paper and electronic copies of this document in whole or in part and declare that the prepared document does not in anyway include copying of previous work on the subject or the use of ideas, concepts, words, or structures regarding the subject without appropriate acknowledgement of the source material.

Signature of Author(s)

.....
Enes ÖZKARTAŞLIOĞLU, Ebrar İNAN

Department of Mechanical Engineering

Certified By.....Assoc. Prof. Barış YILMAZ.....

Project Supervisor, Department of Mechanical Engineering

Accepted By.....

Head of the Department of Mechanical Engineering

ACKNOWLEDGEMENT

First of all, I would like to thank my supervisor Associate Professor. Dr. Barış Yılmaz, for the valuable guidance and advice on preparing this thesis and giving us moral and material support.

June, 2023

Enes Özkarataşlıoğlu,
Ebrar İnan

Table of Contents

1. INTRODUCTION.....	1
1.1. General Information.....	1
1.1.1. Configurations	1
1.2. Components.....	6
1.2.1. Cylinders	7
1.2.2. Pistons.....	7
1.2.3. External Heat Source	7
1.2.4. Gas	7
1.2.5. Cooling Systems.....	7
1.2.6. Flywheel.....	8
1.2.7. Crankshaft.....	8
1.2.8. Regenerator	8
1.2.9. P-v and T-s Diagrams of Stirling Engine	9
1.3. Application of Stirling Engine.....	9
1.3.1. Power Generation.....	9
1.3.2. Combined Heat and Power.....	10
1.3.3. Nuclear Power	11
1.3.4. Automotive Engines.....	11
1.3.5. Aircraft Engines.....	12
1.4. Working Gases in Stirling Engine	13
1.5. Stirling Engine Manufacturers	14
1.6. Solar Stirling Engine.....	15
1.7. Design parameters	17
1.7.1. Solar thermal collectors	17
1.7.2. Thermal Receiver	18
1.7.3. The Reflecting Material.....	18
1.8. Photovoltaic Panels.....	19
1.8.1. Types of photovoltaics (PV) cells	19
1.8.2. Efficiency of solar panels	23
2. METHODOLOGY	24
2.1. STIRLING CYCLE CALCULATIONS.....	24
2.2. Solar Radiation Calculations	32
2.2.1. Latitude Angle (ϕ).....	32
2.2.2. Declination Angle (δ)	32
2.2.3. Hour Angle (ω)	33
2.2.4. Solar Elevation(Altitude) Angle (α)	34
2.2.5. Zenith Angle (ψ).....	34
2.2.6. Solar Azimuth Angle (γ_s).....	35
2.2.7. Solar Radiation.....	35
3. RESULTS	38
3.1. Simulation application on MATLAB software	38
3.2. Effects of hot and cold temperature on efficiency with Stirling and Carnot cycle	39

3.3.	Effects of hot temperature on different gasses	41
3.4.	The effects of regenerator effectiveness with hot temperature variations.....	42
3.5.	Effects of cold temperature of different gasses.....	43
3.6.	The effects of regenerator effectiveness with cold temperature variations	45
3.7.	The effects of regenerator effectiveness.....	46
3.8.	The effects of compression ratio of different gasses	48
3.9.	Effects of solar radiation on Stirling cycle	48
3.10.	Photovoltaic Panel Requirements.....	49
4.	<i>CONCLUSION</i>	51
5.	<i>REFERENCES</i>	53

List of Figures

Figure 1 The schematic views of the configurations [27]	2
Figure 2 The schematic of an alpha configuration [10]	3
Figure 3 The schematic of a beta configuration [28]	4
Figure 4 The schematic of gamma configuration [29]	5
Figure 5 Different models of gamma configuration [44]	5
Figure 6 Components of the Stirling engine.....	6
Figure 7 (a) Operating principal SE (b) P-v T-s Diagrams for SE and Carnot cycles [3].....	9
Figure 8 Solar Powered Stirling Engine [15]	10
Figure 9 Structural Schematic Diagram of a Free Piston Stirling Engine System.....	10
Figure 10 1979 NASA AMC w/ Stirling Engine [2].....	12
Figure 11 Data results for CSSE model for different variables [8]	13
Figure 12 Effect of Stirling compression ratio on different parameters [8]	14
Figure 13 The parabolic dish with Stirling engine [45]	15
Figure 14 SSE and cross-section of PCU	15
Figure 15 The power conversion unit.....	16
Figure 16 The types of solar collector [5]	17
Figure 17 Monocrystalline solar panel [34]	20
Figure 18 Manufacturing process of mono- and poly-crystalline solar panels [35].....	21
Figure 19 Polycrystalline solar panel [34].....	22
Figure 20 Amorphous silicon (thin-film) solar panel [43]	23
Figure 21 Efficiency of solar panels between 2006-2019 [43]	24
Figure 22 Thermodynamic processes of the Stirling cycle [33].....	25
Figure 23 Thermodynamic processes of the cycle [32].....	25
Figure 24 P-v diagram of the Stirling Engine	30
Figure 25 Scheme of latitude [31]	32
Figure 26 Declination angle vs. day number graph with three formulas	33
Figure 27 Illustration of zenith, altitude and azimuth angle [30]	35
Figure 28 The comparison of process of solar radiations.....	37
Figure 29 The interface of the simulation application on MATLAB.....	38
Figure 30 Outputs of the application	38
Figure 31 P-V diagram of Stirling cycle	39
Figure 32 The variations of total input heat against hot temperature for different working gas.....	40
Figure 33 The variations of total input heat against cold temperature for different working gas types.	40
Figure 34 The variations of total input heat against hot temperature for different gasses	41
Figure 35 The variations of efficiency against hot temperature for different gasses	41
Figure 36 The variations of net work against hot temperature.....	42
Figure 37 The variations of total input heat against hot temperature for regenerator effectiveness	43
Figure 38 The variations of efficiency against hot temperature for regenerator effectiveness	43
Figure 39 The variations of total input heat against cold temperature for different gasses	44
Figure 40 The variations of efficiency against cold temperature for different gasses	44
Figure 41 The variations of net work against cold temperature	45
Figure 42 The variations of total input heat against cold temperature for regenerator effectiveness	45
Figure 43 The variations of efficiency against cold temperature for regenerator effectiveness	46
Figure 44 The variations of total input heat against regenerator effectiveness with different gasses....	47
Figure 45 The variations of efficiency against regenerator effectiveness with different gasses.....	47
Figure 46 The variations of total input heat against compression ratio for different gasses.....	48
Figure 47 The variations of extraterrestrial solar radiation against month	49
Figure 48 The variations of terrestrial solar radiation against month	49
Figure 49 The variation of panel area against hot temperature of different gasses.....	50
Figure 50 The variation of panel area against compression ratio of different gasses	51

ABSTRACT

Solar Powered Stirling Engine

In this thesis, at the beginning, the history and working principle of Stirling engine and James Stirling's studies are investigated. With the usage of this informations, configurations and the components of the engine are investigated individually to understand what the main purpose of usage of Stirling engine is. With the application Stirling engines, some diagrams are examined with the help of theoretical background of the engine. By using Stirling engine informations, the study was converted into "Solar Powered Stirling Engine" to investigate more detail about the topic. In the following, solar concentrators, and their parameters such as diameter or reflecting materials are investigated. Also, to understand the working principle of solar Stirling engine, its components with the details and properties are investigated. In addition, since design parameters play important role on solar Stirling engine, these parameters are defined.

After the literature study and collecting theoretical information, some diagrams and tables are obtained according to the research. It is observed that with different compression ratios and working fluids such as Helium, air, C₂H₂ or Ne, the efficiency, dish area or piston volume can change. In solar powered Stirling engine, power conversion unit has different structural elements to run the system properly. Also, this power conversion unit has cooling system working with water but water consumption is very low. This reduces the water footprint. Moreover, the concentrator's diameter affects the the amount of collected solar energy and accordingly the heat energy absorbed by the receiver. The reflecting material consists of more than one layer which are glass and covering material, for instance, silver or aluminum.

Keywords: Stirling Engine, Solar Stirling Engine, Dish Concentrator, Power Conversion Unit

SYMBOLS

C_r : Geometric concentration ratio

α : Rod angle

ϕ : Latitude angle

δ : Declination angle

ω : Hour angle

α : Elevation (altitude)

γ : Solar Azimuth Angle

ψ : Zenith angle

Q_s : The amount of heat supplied

Q_r : The amount of heat released

Q_{net} : The amount of net heat

ABBREVIATIONS

BDC : Bottom Dead Center

CHP : Combined Heat and Power

CSSE : Concentrated Solar Stirling Engine

CSP : Concentrating Solar Power

PCU : Power Conversion Unit

PSDC : Parabolic Solar Dish Concentrator

SE : Stirling Engine

SSE : Solar Stirling Engine

TDC : Top Dead Center

1. INTRODUCTION

In this report, it is aimed to examine the Stirling engine by integrating with the solar energy. Required information is obtained from literature research from articles about history, components, working principle of Stirling engine and also application areas, working fluid etc. With the help of these theoretical information, the solar powered Stirling engine will be considered for the investigation.

1.1. General Information

In 17th century, hot air engines are started using in the world. Hot air engines were dangerous in terms of high pressure levels. Because they have tendency to explode and damage the environment. To prevent these kinds of accidents, studies have started by scientists. In 1816, Scottish father Reverent Robert Stirling invented first closed-cycle hot air engine which is called Stirling engine. His brother James Stirling has played a role of research and developments of the Stirling engine.

Stirling engine is an external combustion engine used for different purposes. The heating and cooling the isolated working fluids runs the engine. Between different temperatures, due to the increasing and decreasing in the pressure of the working fluid, cyclic compression and expansion moves occur. Thus, the engine works with the conversion of heat energy to mechanical energy.

1.1.1. Configurations

Stirling engine has several types of configurations which are necessary in terms of the purpose of usage field. Alpha, Beta and Gamma types are the most common configurations and each has different components, geometries, efficiencies. These configurations give a chance to select the appropriate one based on what it is used for or where it is used. Because each configuration has different geometries or positions which are arranged to be suitable for the requirements.

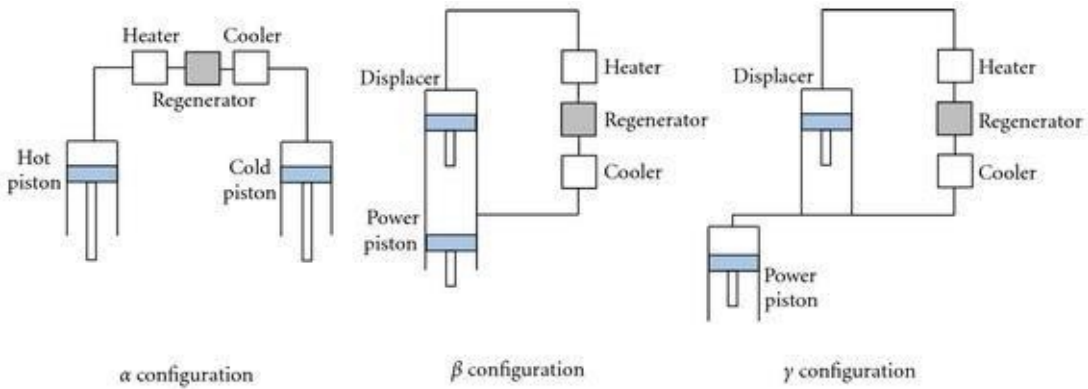


Figure 1 The schematic views of the configurations [27]

1.1.1.1. Alpha Configurations

It consists of one flywheel, two heat exchanger in hot cylinder and cold cylinder and two power pistons, one in hot cylinder and the other one is in cold cylinder. The working fluid is driven between these two pistons by expansion and compression. The connecting rods of two pistons are connected in the same flywheel. Due to the moves of pistons, flywheel creates a work output. Alpha type has high power-to-volume ratio. Because of the fact that there is high temperature of piston, the Alpha-type engine has some technical problems.

The working principal bases on volume changes of the system and pressure differences in each cylinder due to the temperature. Most of the working fluid is in hot cylinder at the beginning. Due to the contact with the cylinder's wall, it is heated, its pressure increases and it expands. The volume of the system increases because of the expansion into cold cylinder. When the gas transferred to the cold cylinder, the system has its maximum volume. The gas cools down and its pressure decreases. Due to the momentum of flywheel, the piston in hot cylinder begins moves inward and reduces the volume of the system.

Until the all working fluid reaches the cold side, cooling continues. The cold cylinder has its maximum volume and hot cylinder has its minimum. Then, because of that the cold cylinder begins compression, the volume of system keeps decreasing. The system reaches its minimum volume and hot cylinder starts expansion. Thus, the cycle is repeated.

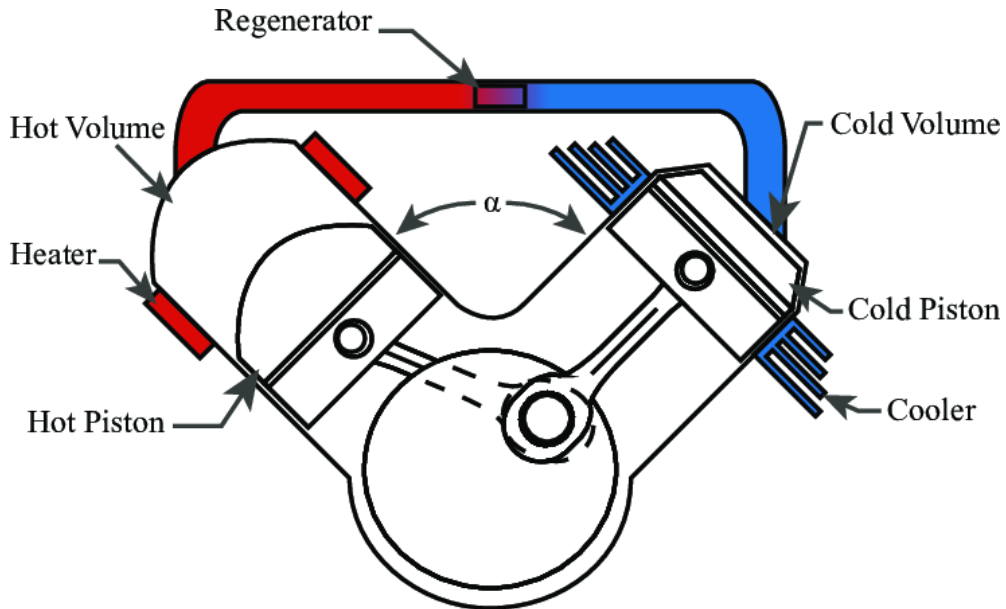


Figure 2 The schematic of an alpha configuration [10]

1.1.1.2. Beta Configurations

In this configuration, the system contains a flywheel, one hot and one cold heat exchanger, one power piston and one displacer piston which is in the same cylinder with the power piston. Displacer piston is loose fit and it causes the back and forth moves of the working fluid between the hot and the cold heat exchanger. The rod of displacer piston passes through power piston. Also, the displacer must be 90 degrees ahead of the power piston. Unlike the alpha configuration, beta configuration does not have technical problems like high temperature of piston. Because the power piston has no contact with the hot side. First, power piston compresses the working fluid and the displacer moves to make the most of the gases reach the hot heat exchanger. In hot exchanger, the gas is heated and its pressure increases. This pushes the power piston to the top point of the stroke. The displacer moves to shuttle the working fluid to the cold end of the cylinder. Due to the momentum of the flywheel, the cooled gas is compressed.

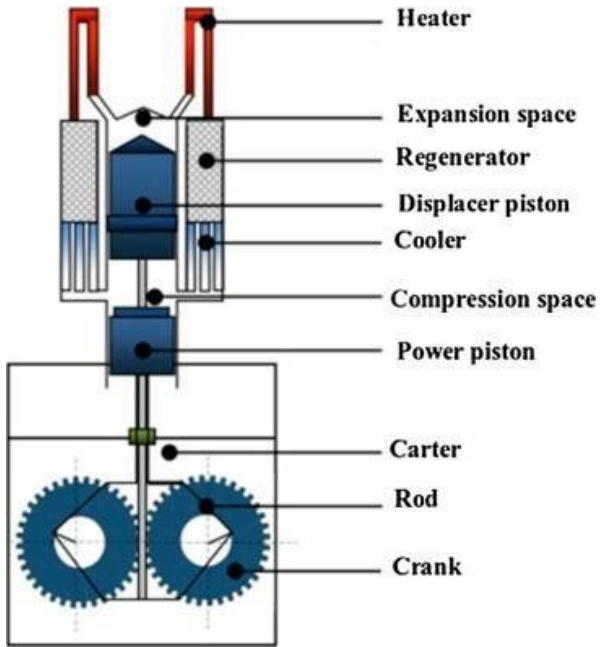


Figure 3 The schematic of a beta configuration [28]

1.1.1.3. Gamma Configurations

Gama configuration is similar to the beta configuration. It consists of a flywheel, a power piston, a displacer and two different cylinders unlike the beta configuration. The power piston is in different cylinder from the displacer but they are still connected to the same flywheel, shown in Figure 4. The reason of separating the cylinders is to produce lower compression ratio. Using different cylinders are mechanically simpler. According to the researchers, theoretically, the gamma configuration has the highest efficiency compared to the alpha and beta configurations. Gama type is classified in four groups as Lauberau- Schwartzkopff, Heinrici, Rainbow and Robinson. Each class has different positioning structure in terms of cylinders, pistons and regenerators. For instance, the cylinders are parallel to each other or there are two expansion cylinders. In Heinrici type gamma configuration, the regenerator is an external regenerator. These differences are demonstrated below in Figure 5.

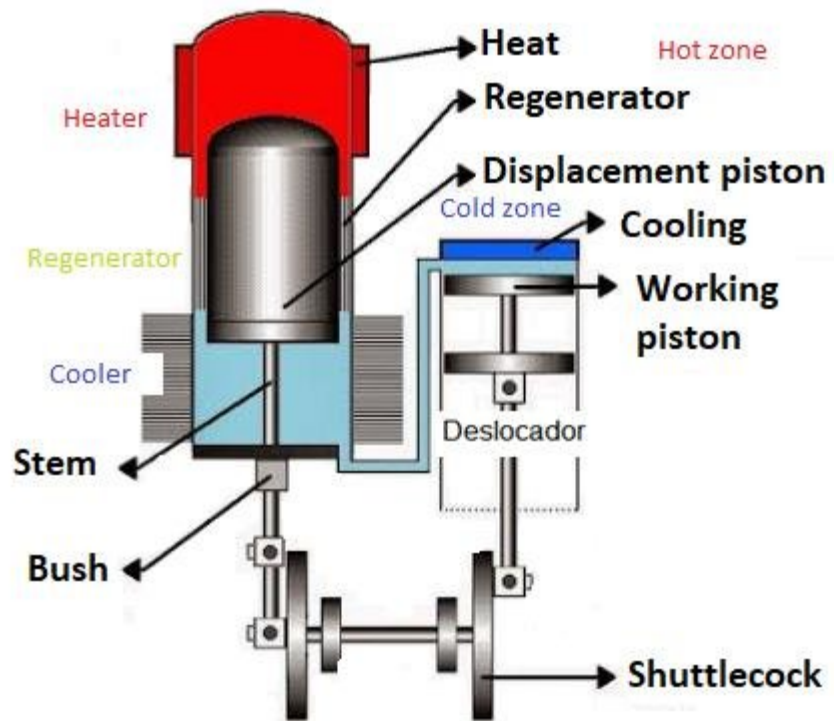


Figure 4 The schematic of gamma configuration [29]

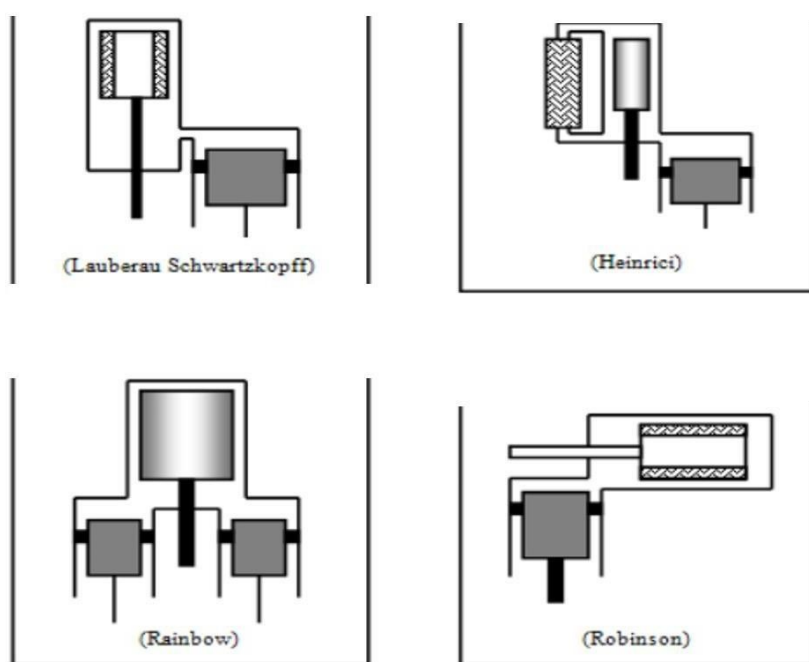


Figure 5 Different models of gamma configuration [44]

1.2. Components

There are several main parts of a Stirling Engine:

1. Cylinders
2. Pistons
3. External Heat Source
4. Gas
5. Cooling System
6. Flywheel
7. Crankshaft
8. Regenerator

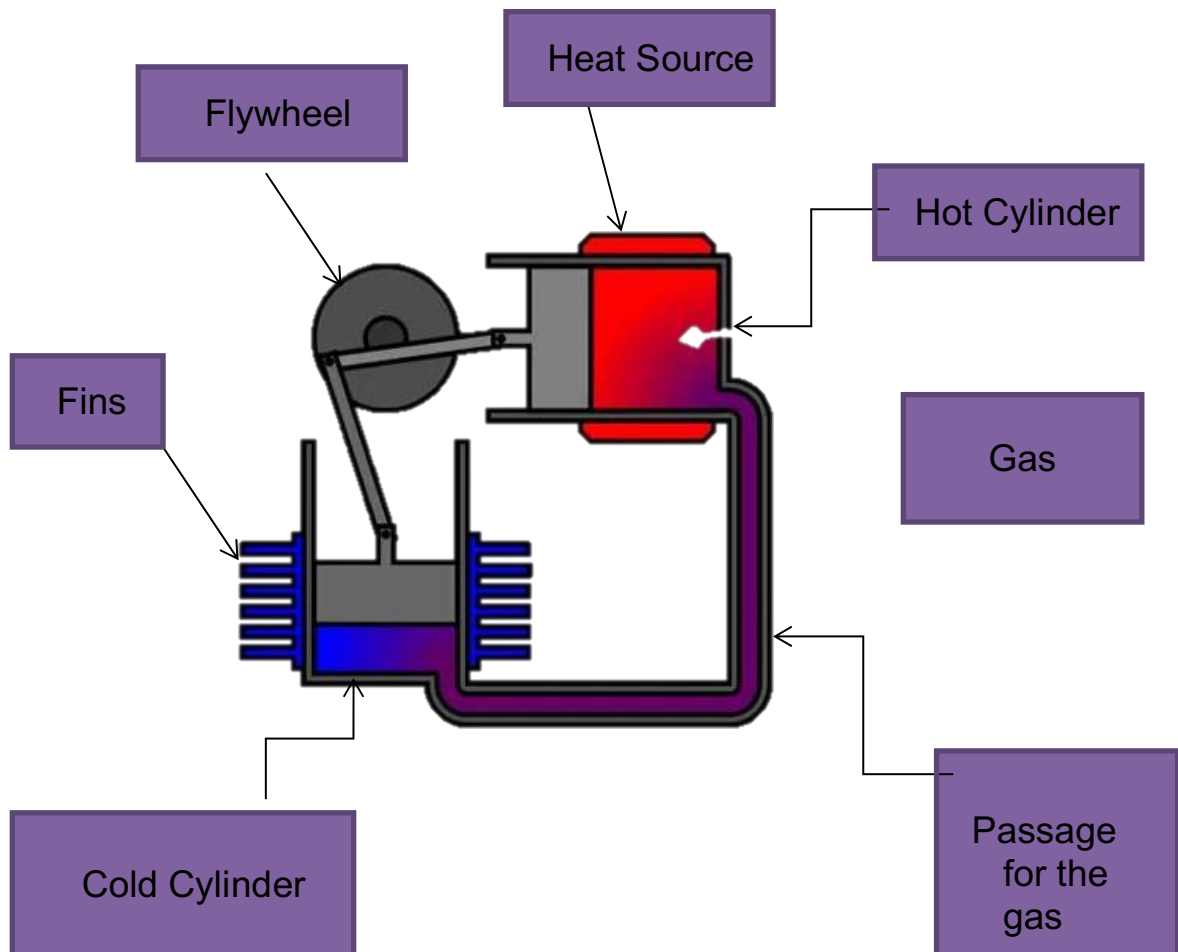


Figure 6 Components of the Stirling engine

1.2.1. Cylinders

Depending on whether it is an alpha or a beta Stirling engine, a Stirling engine uses 1 or 2 cylinders.

The Alpha Stirling Engine utilizes two cylinders that are;

A cold wall cylinder- It is the cylinder that provides cooling of the gas by some external means like cooling system, in order to reuse the gas for another cycle.

A hot wall cylinder- It is the cylinder through which the external heat source is connected that provides heat to the gas inside this cylinder in order to expand the gas.

1.2.2. Pistons

The final power output of the engine is produced by the rigid cylindrical piston that is employed inside the cylinder.

One or two pistons, depending on whether it is an alpha or beta Stirling engine, are used.

1.2.3. External Heat Source

In order to drive the piston, an external heat source (either renewable or non-renewable) is utilized to heat the hot cylinder's wall (Alpha SE) or hot end (Beta SE). This causes the gas to expand by increasing the potential energy of the gas molecules.

1.2.4. Gas

The Stirling engine's working fluid, a gas, is employed inside the cylinder in a way that causes the pistons to move back and forth as a result of the gas's compression and expansion.

The channel that connects the two cylinders of the alpha Stirling engine allows the gas to travel from the cold cylinder to the hot cylinder and back again.

In a beta Stirling engine, a loosely fitting displacer powered by the flywheel of the engine transfers gas between the cold and hot ends of the cylinder.

1.2.5. Cooling Systems

The Stirling engine's working fluid, a gas, is employed inside the cylinder in a way that causes the pistons to move back and forth as a result of the gas's compression and expansion.

The channel that connects the two cylinders of the alpha Stirling engine allows the gas to travel

from the cold cylinder to the hot cylinder and back again.

In a beta Stirling engine, a loosely fitting displacer powered by the flywheel of the engine transfers gas between the cold and hot ends of the cylinder.

1.2.6. Flywheel

Same as the IC engine a flywheel is used at the outer part of the crankshaft to store the engine's output for further transmission.

1.2.7. Crankshaft

It is the shaft that allows the piston to transmit mechanical work to the flywheel.

The flywheel's final output is rotating motion, which is created from the piston's reciprocating action.

Through the crank pins, the pistons from the cold and hot cylinders of the alpha Stirling engine are connected to the crankshaft.

1.2.8. Regenerator

A regenerator is located between the heater and cooler and provides pre-heating and pre-cooling for the heat entering the heater and cooler.

The regenerator boosts the Stirling Engine's effectiveness. The regenerator lowers system and fuel costs. However, using it is not required.

1.2.9.P-v and T-s Diagrams of Stirling Engine

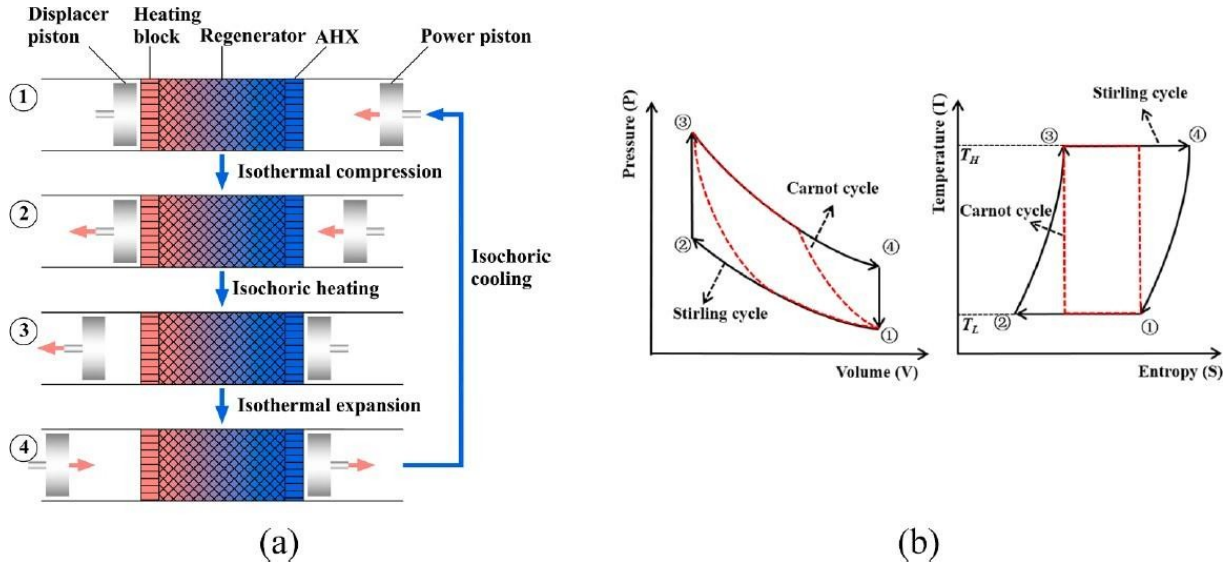


Figure 7 (a) Operating principle SE (b) P-v T-s Diagrams for SE and Carnot cycles [3]

As it's seen on the graphs, there are similarities between Carnot cycle and Stirling cycle. Not only both systems have fundamentally similar configuration, but also they are differences such as Carnot cycle has two adiabatic process apart from the heat addition ones, the Stirling cycle has two isochoric process. According to graph, we can recommend about cycles,

Stirling cycle needs constant volume due to increasing pressure after a point but Carnot cycle increases parabolic by volume in P-v Diagram. In T-s diagram, Carnot cycles needs constant entropy due to increasing temperature but Stirling cycle increase temperature by increasing entropy.

1.3. Application of Stirling Engine

1.3.1. Power Generation

A Stirling engine placed at the center of a parabolic mirror has a conversion efficiency that is higher than non-concentrated photovoltaic cells and lower than concentrated photovoltaics.

These systems, on a 19 km² solar farm will use mirrors to direct and concentrate sunlight onto the engines which will in turn drive generators. According to research "a large, tracking, concentrating solar power (CSP) dish collector that generates 25 kilowatts (kW) of electricity in full sun. Each of the 38-foot-diameter collectors contains over 300 curved mirrors (heliostats)

that focus sunlight onto a power conversion unit, which contains the Stirling engine. The dish uses dual axis tracking to follow the sun precisely as it moves across the sky.[15]



Figure 8 Solar Powered Stirling Engine [15]

1.3.2. Combined Heat and Power

In a combined heat and power (CHP) system, mechanical or electrical power is generated in the usual way, however, the waste heat given off by the engine is used to supply a secondary heating application. This can be virtually anything that uses low-temperature heat. It is often a pre-existing energy use, such as commercial space heating, residential water heating, or an industrial process.

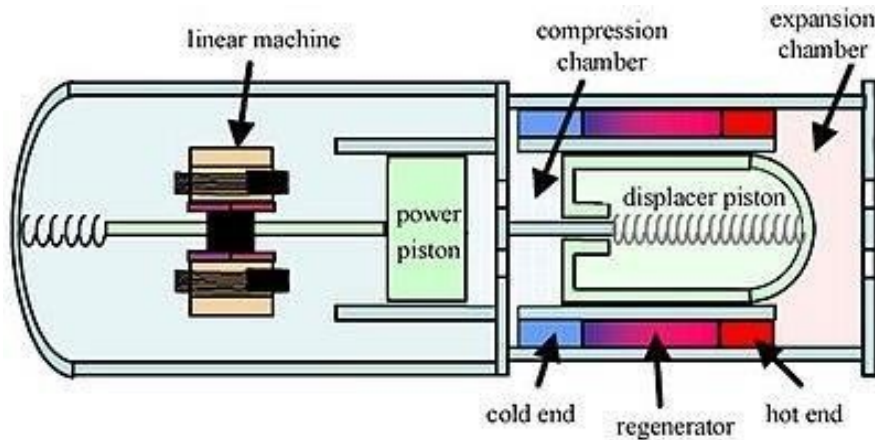


Figure 9 Structural Schematic Diagram of a Free Piston Stirling Engine System

Thermal power stations on the electric grid use fuel to produce electricity. However, there are large quantities of waste heat produced which often go unused. In other situations, high-

grade fuel is burned at high temperatures for a low-temperature application. According to the second law of thermodynamics, a heat engine can generate power from this temperature difference. In a CHP system, the high-temperature primary heat enters the Stirling engine heater, then some of the energy is converted to mechanical power in the engine, and the rest passes through to the cooler, where it exits at a low temperature. The "waste" heat actually comes from the engine's main cooler, and possibly from other sources such as the exhaust of the burner, if there is one.

The power produced by the engine can be used to run an industrial or agricultural process, which in turn creates biomass waste refuse that can be used as free fuel for the engine, thus reducing waste removal costs. The overall process can be efficient and cost-effective.

1.3.3.Nuclear Power

Nuclear power facilities' steam turbines could be replaced with Stirling engines, which would streamline the facility, increase efficiency, and decrease radioactive waste. Liquid sodium is used as a coolant in a number of breeder reactor types. A water/sodium heat exchanger is necessary if the heat is to be used in a steam plant, which raises some questions in the event of a leak given how aggressively sodium reacts with water. Water is not required at any point in the cycle when using a Stirling engine. For nuclear plants in dry regions, this would be beneficial.

1.3.4.Automotive Engines

It is often claimed that the Stirling engine has too low a power/weight ratio, too high a cost, and too long a starting time for automotive applications. They also have complex and expensive heat exchangers. A Stirling cooler must reject twice as much heat as an Otto engine or Diesel engine radiator. The heater must be made of stainless steel, exotic alloy, or ceramic to support high heating temperatures needed for high power density, and to contain hydrogen gas that is often used in automotive Stirlings to maximize power. The main difficulties involved in using the Stirling engine in an automotive application are startup time, acceleration response, shutdown time, and weight, not all of which have ready-made solutions.[4]

Automobiles had powered by Stirling engines were developed in test projects by NASA. Engines not only developed by NASA but also Ford Motor Company using engines provided by Philips and by American Motors Corporation (AMC). NASA designated MOD I and MOD II.

MOD I was achieved with equal power spark ignition engine and design continued to

exhibit a shortfall in fuel efficiency. In addition to this, there were two important drawbacks for consumers; first was the time needed to warm up – because most drivers do not like to wait to start driving; and second was the difficulty in changing the engine's speed – thus limiting driving flexibility on the road and traffic. The process of auto manufacturers converting their existing facilities and tooling for the mass production of a completely new design and type of powerplant was also questioned. [11]



Figure 10 1979 NASA AMC w/ Stirling Engine [2]

The MOD II project in 1980 produced one of the most efficient automotive engines ever made. The engine reached a peak thermal efficiency of 38.5%, compared to a modern spark-ignition (gasoline) engine, which has a peak efficiency of 20-25%. The Mod II project replaced the normal spark-ignition engine in a 1985 4-door Chevrolet Celebrity notchback. Startup time in the NASA vehicle was a maximum of 30 seconds, while Ford's research vehicle used an internal electric heater to quickly start the engine, giving a start time of only a few seconds. The high torque output of the Stirling engine at low speed eliminated the need for a torque converter in the transmission resulting in decreased weight and transmission drivetrain losses negating somewhat the weight disadvantage of the Stirling in auto use. This resulted in increased efficiencies being mentioned in the test results. The experiments indicated that the Stirling engine could improve vehicle operational efficiency by ideally detaching the Stirling from direct power demands, eliminating a direct mechanical linkage as used in most current vehicles.[7]

1.3.5. Aircraft Engines

Robert McConaghy created the first flying Stirling engine-powered aircraft in August 1986. The Beta type engine weighed 360 grams and produced only 20 Watts of power. The engine was attached to the front of a modified Super Malibu radio control glider with a gross

takeoff weight of 1 kg. The best-published test flight lasted 6 minutes and exhibited. [6]

1.4. Working Gases in Stirling Engine

The proposed working gases in this study are classified into main three categories according to their chemical structure:

- Monatomic gases (Helium-He, Argon-Ar, Neon-Ne, Krypton-Kr, Xenon-Xe).
- Diatomic gases (Air, Hydrogen-H₂, Nitrogen-N₂).
- Polyatomic gases (CO₂ (Carbon dioxide) , NH₃ (Ammonia), CH₄ (Methane), C₂H₂ (Acetylene))

The literature made it extremely evident that air and/or helium were usually applied in solar dish Stirling engines. However, in this study, a spot light is focused on the effect of using different gases with different heat capacities for engines. Different heat capacities have a great influence on the compression and presser ratios hence the efficiency. In this work, the selection of the working gas is performed based on some important criteria such as;

Maximum engine efficiency, maximum compression and pressure ratios, Minimum dish area and maximum dish concentration ratio, Minimum cost issues related to the engine and the dish area, Availability of the gases for industrial issues, Flammability, explosion, and environmental impact.[8]

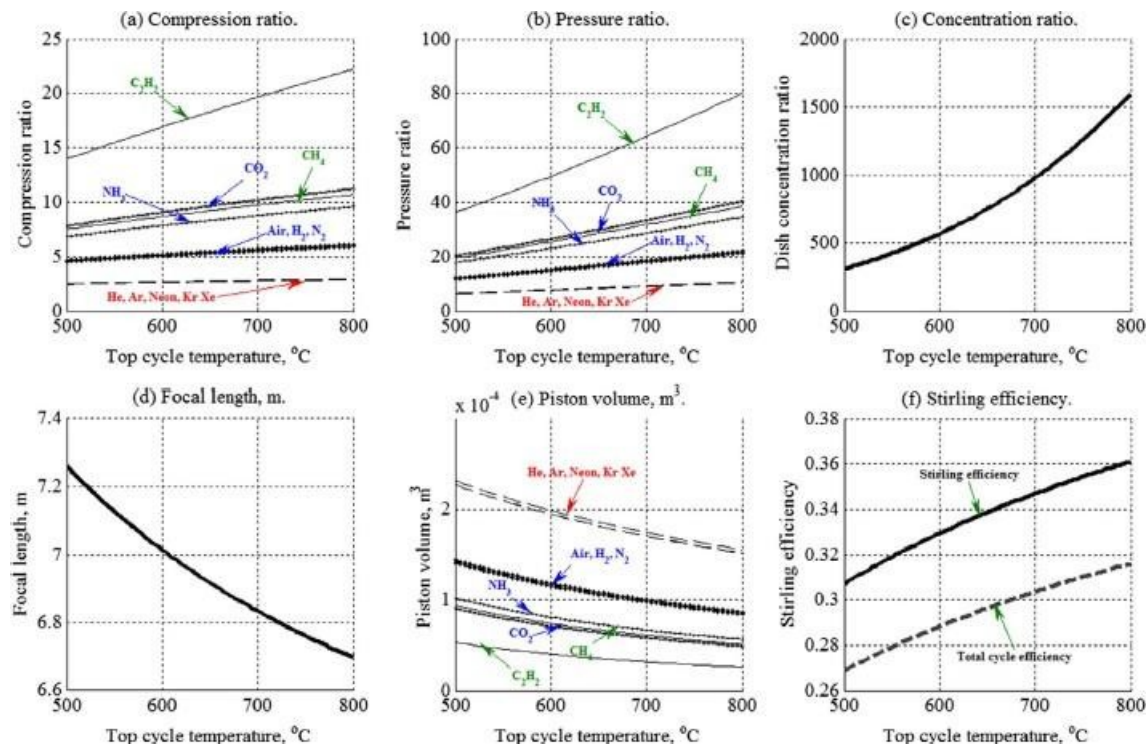


Figure 11 Data results for CSSE model for different variables [8]

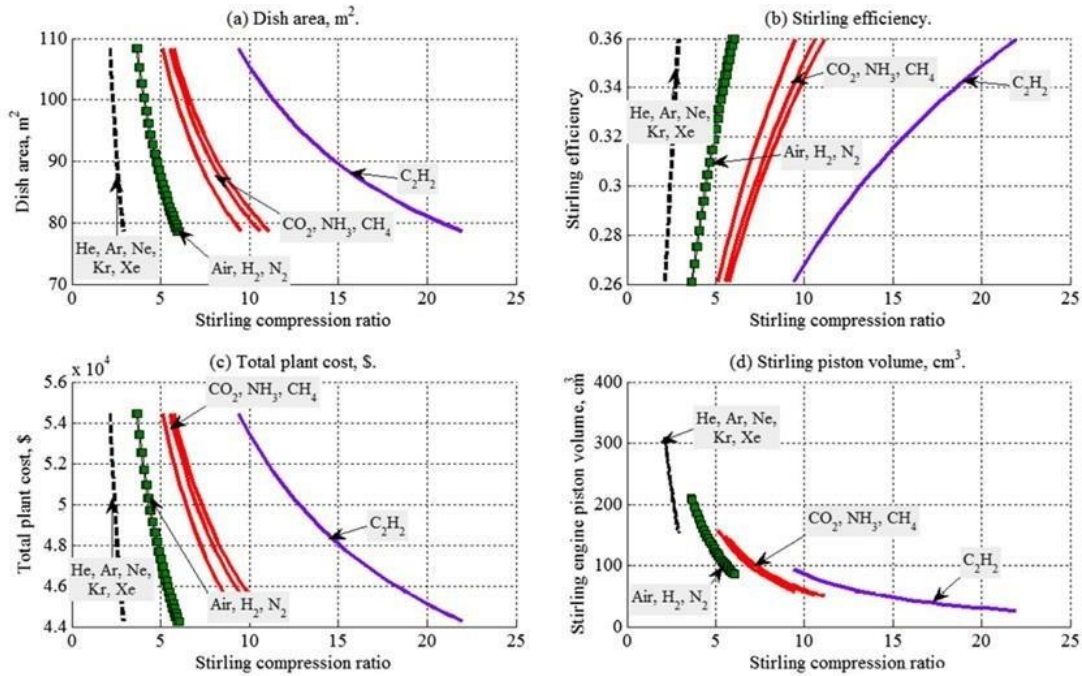


Figure 12 Effect of Stirling compression ratio on different parameters [8]

According to Figure 12 there are several parameters to select using gases for Concentrated Solar Stirling Engine. The most common use gases are air and helium. This may be cause of the high efficiency in low compression ratio. Moreover, low compression ratio has not only provided high efficiency but also it leads to decrease total plant cost. As we mentioned before, these are a couple of criteria to choose the gases in the Stirling engine, it would select regarding plant needs.

1.5. Stirling Engine Manufacturers

After examination of the manufacturers of the Stirling engine, we conclude that manufacturing of Stirling engine does not significant in Turkey. Even Turkey does not manufacture SE, there are several manufactures around the world that we found. These are;

FRAUSCHER THERMAL MOTORS

(GERMANY) AZELIO AB

(SWEDEN)

STIRLING CRYOGENICS (REVERSE

STIRLING)(NETHERLANDS) AMETEK SUNPOWER

INC. (USA)

1.6. Solar Stirling Engine

In 1870, when the Stirling engine is ready to operate with solar energy, the first solar powered Stirling engine was invented. It was an open cycle hot-air engine. There were a parabolic mirror which is used as concentrator to heat the steam and use it for driving the Stirling engine.

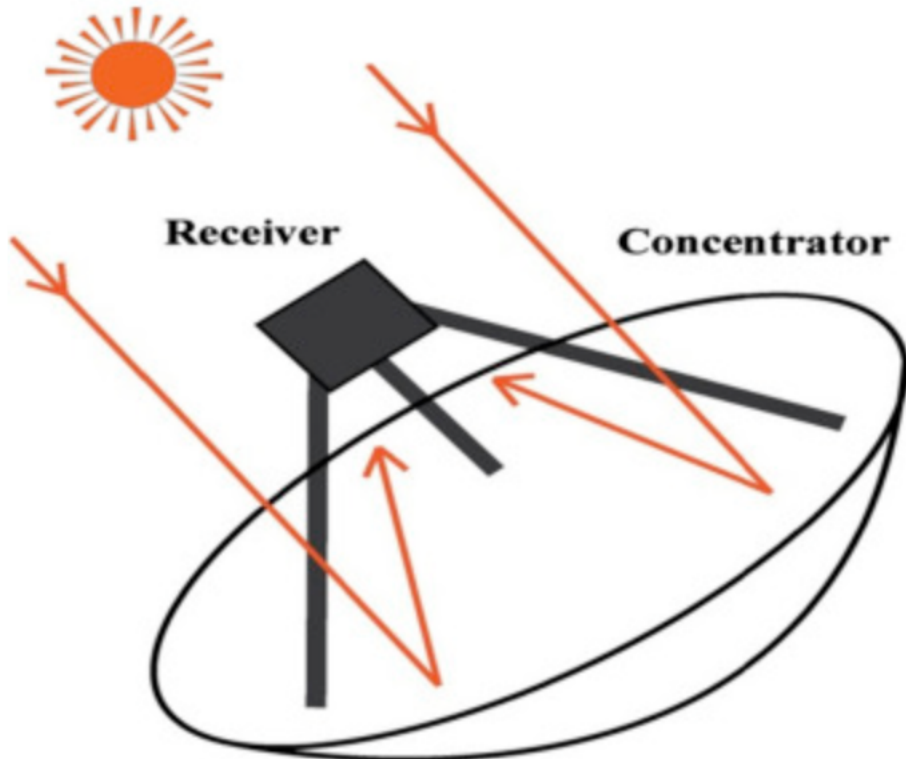


Figure 13 The parabolic dish with Stirling engine [45]

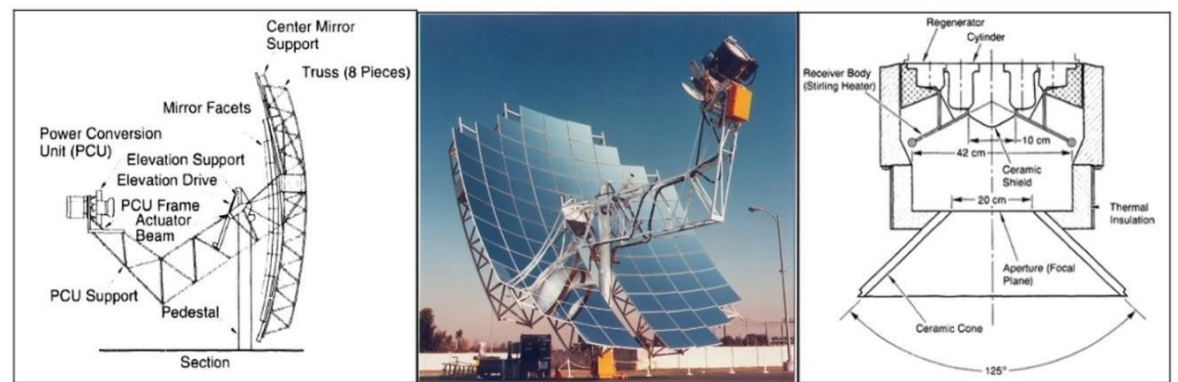


Figure 14 SSE and cross-section of PCU

The dish systems use a parabolic mirror to reflect and concentrate incoming direct normal sun rays to focal point where the power conversion unit (PCU) is placed. Inside PCU, there is

a cavity which contains the receiver to absorb the heat from concentrated radiation. These concentrated radiations were obtained by the sun rays. The PCU is consisting of cavity into which the sun rays are concentrated, receiver which absorbs the heat from concentrated radiation and transfers to Stirling engine. [46]

The power conversion unit contains the Stirling engine with generator and receiver which plays role as an external heat exchanger. The thermal receiver is a set of thin tubes with a working fluid such as Helium. The thermal receiver plays a role as if it was a bridge to transfer heat from concentrated radiation from obtained from solar dish into the hot area of the Stirling engine placed in upper side. The research demonstrates that the receiver absorbs the incoming thermal energy which is in range of $700^{\circ}\text{C} - 800^{\circ}\text{C}$. In expansion cylinder, heat energy absorbed in working fluid which is approximately 650°C is converted into mechanical energy. There is also a cooling system for PCU and the engine which is a closed loop cooling system to minimize the water consumption in the engine. Cooling is carried out by an air fan and a cooler inside the PCU. At input of the engine, the temperature of cooling liquid which is called anti-freeze fluid is about 45°C . Water is only used for cleaning the solar concentrator's surface which causes significantly low usage of water. In addition, to regulate and control the whole system, switchboard and control systems are placed. Also, there is a pressure vessel with working fluid and protective shield to provide heat resistance by ceramic.

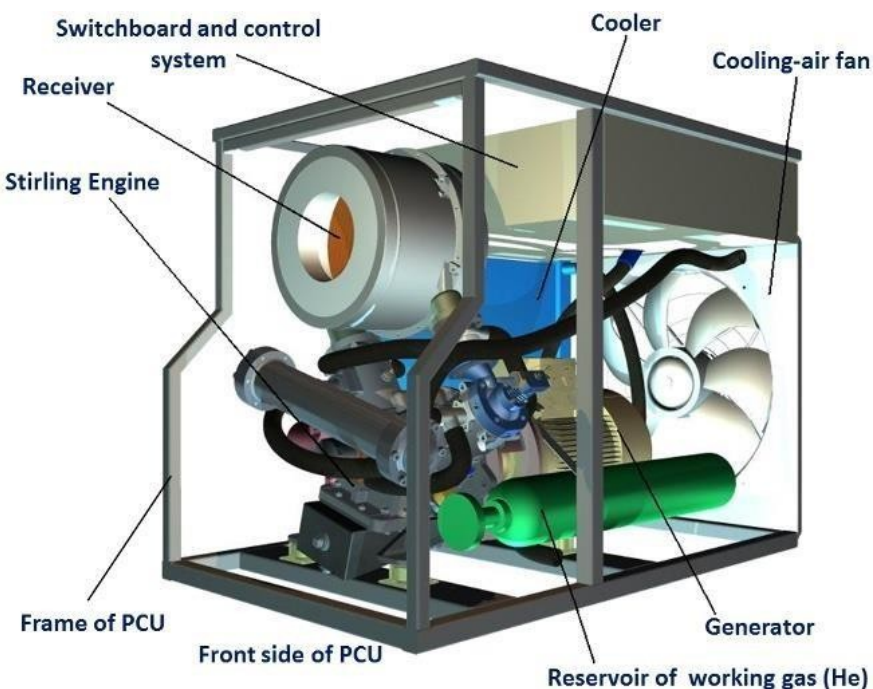


Figure 15 The power conversion unit

1.7. Design parameters

1.7.1. Solar thermal collectors

The main duty of the solar collector is to concentrate the radiations from sun and convert them into usable energy. Due to some losses in terms of thermal and optic, The solar collectors can be classified in two main classes which are the focusing and the non- focusing also called flat collectors. The concentrating solar collectors work at very high temperatures compared to the flat collectors. Therefore, they are typically joined with different thermal systems. The efficiency of the collector changes with respect to the concentration ratio (C_r) of the solar collector. The formula of concentration ratio:

$$C_r = \frac{\text{Area of aperture}}{\text{Area of receiver}} \quad (1)$$

When the concentration ratio is greater than one ($C_r > 1$), it represents the concentration collectors. If the ratio is equal to zero ($C_r = 0$), it demonstrates that the collector type is flat collector (non-focusing). In case of the fact that C_r is greater than 5, then the solar concentrators are called imaging concentrating collectors. If less than 5, it is called the non- imaging collectors. The classification of solar collectors is demonstrated below, in figure 16.

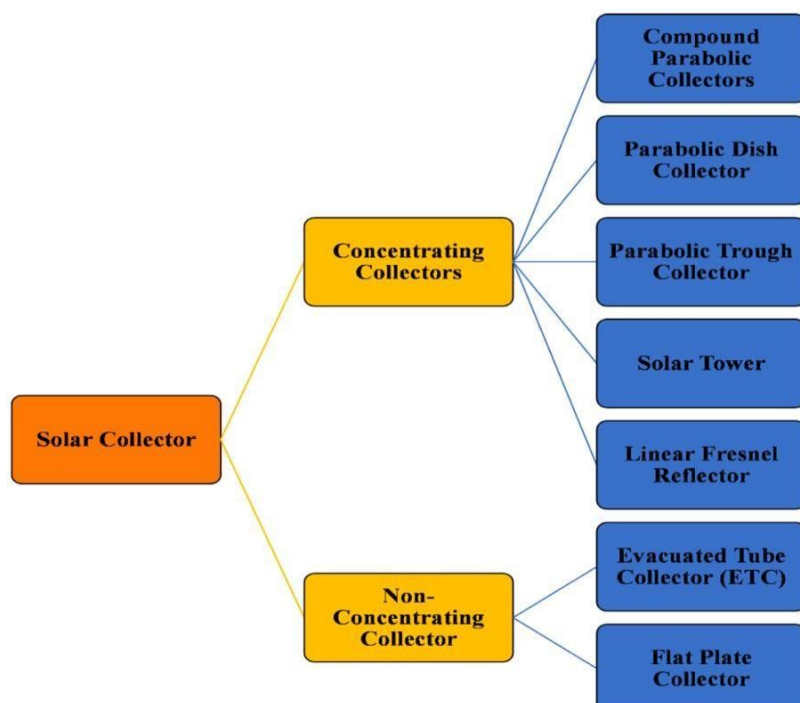


Figure 16 The types of solar collector [5]

To concentrate the radiations coming from the sun to the engine, the solar powered Stirling engine contains a parabolic reflector. The parabolic mirror is fixed using metal sheet on the structure. The receiver may have different geometries in the dish concentrator such as hemispherical, cubical or spiral etc. The main reason why the concentration ratio of PSDC is between 100 and 500 is to reach high temperatures in the solar collector. Some parameters have to be taken into account when designing a PSDC which are focal length, aperture diameter and rim angle.

The research shows that the diameter of a parabolic solar dish is between 3 and 10 meters. In terms of material, it includes some segments of fiberglass and reflecting material. Material will be discussed incoming sections. Moreover, there are ribs and rings in the structure of the collector. To reach the minimum weight of the dish, their sizes are minimized. This situation also decrease the stress on the beams and accordingly the deflection. [9]

1.7.2. Thermal Receiver

The receiver, which is positioned at the focal point of the concentrator, must receive the concentration of solar radiations in order to reach the necessary thermal temperature. In order to capture the most solar thermal energy, the SE and plates which absorb the heat are often placed at the focal point of the cavity receiver. Therefore, a cavity receiver needs to be placed at the dish's focus in order to reduce convection and radiation losses.

1.7.3. The Reflecting Material

Table 1 Properties of the reflecting materials [5]

Used material	Reflectivity (%)	Emissive (%)	Working temp (°C)
Aluminum	90	10	98
Aluminum, Acrylic	98	2	95
Aluminum Acrylic, Silver	97	3	125
Silver, Acrylic	95	5	100
Polyethylene, Aluminum	97	3	100
Polyethylene, Aluminum	97	3	100
Alumina, Copper, Polymer, Silvered	97	3	95
The Ceramic, metallic covering film	95	5	90

When designing a solar concentrator, the reflecting material should be chosen carefully. To be able to reflect the maximum solar radiation, the concentrator must have the most appropriate material properties. There are different parameters according to the material choice. One is the reflectivity of solar concentrator which represents the amount of the reflected solar radiations to the receiver. From Table 1, it is concluded that the aluminum and silver plates are often used by covering the first layer of the dish which is plastic or glass. With the first studies, determination process for the thickness of reflecting mirrors to reflect solar rays, it is decided that the thickness should be between 1- mm and 4 mm with the material of silver. After some research and development of the topic, it is observed that silver mirrors which have 1-mm thickness provides the most reflective performance.[9] Since polymer films are inexpensive, many designers have used thin polymer layers that have been covered with silver or aluminum.

1.8. Photovoltaic Panels

Solar energy is utilized to generate electricity through photovoltaic (PV) panels. PV panels are made up of a number of separate cells that are joined together to generate power at a specific voltage. DC devices by nature are photovoltaic panels. They require the usage of an inverter to generate AC. Up to a specific voltage, PV cells produce current proportionally to the amount of solar energy. The power from a PV cell will keep increasing until the current starts to decrease since power is proportional to the product of current and voltage. A PV panel has numerous cells connected in series since the maximum voltage from individual cells is less than 1 V. Over the course of a year and a day, the actual radiation level at any given location on the earth's surface will change dramatically. All photovoltaic (PV) cells are composed of many layers of silicon in terms of composition. [13]

1.8.1.Types of photovoltaics (PV) cells

It was already noted that silicon, a semi-conducting semiconductor, is used to make solar panels. According to Chen and Wang [14], when a semi-conducting material is exposed to the sun beam, a direct electrical current is produced and transported through the use of metal conductors. A solar panel is made up of a number of solar cells that are connected together in order to produce a big current from the system [15]. Then, these panels are enclosed by a glass panel to create a PV system out of a collection of modules. The best electrical output can then be produced as needed by connecting these systems.

1.8.1.1. Amorphous Silicon (Polycrystalline (Multicrystalline) and Monocrystalline Silicon)

These components are utilized to create a variety of panels, each with unique properties

and results [40]. For instance, polycrystalline or monocrystalline silicon is the primary component of first-generation solar cells. Second generation silicon icons, however, are made of amorphous material. According to Ullal [13], these materials have made it possible for second-generation solar panels to utilize thin semi-conductor silicon layers to create effective solar cells in terms of thin films at a reasonable price.

1.8.1.2. Monocrystalline silicon

These panels are made from a single silicon crystal that can be divided into cells. This kind of material is used to make the solar cells, which are thought to be the most effective photovoltaic technology. The solar panels made of this material have a conversion efficiency that can range from 15 to 25 percent [16].

The cells are typically made in the shape of octagons and are black in color. In order to create a system for pumping water, Nogueira [17] employed monocrystalline solar panels, which he found to have an efficiency of about 10%—close to 3% greater than the polycrystalline panel used in the experiment. A monocrystalline solar panel is depicted in Figure 17 below, while a polycrystalline panel is depicted in Figure 19.

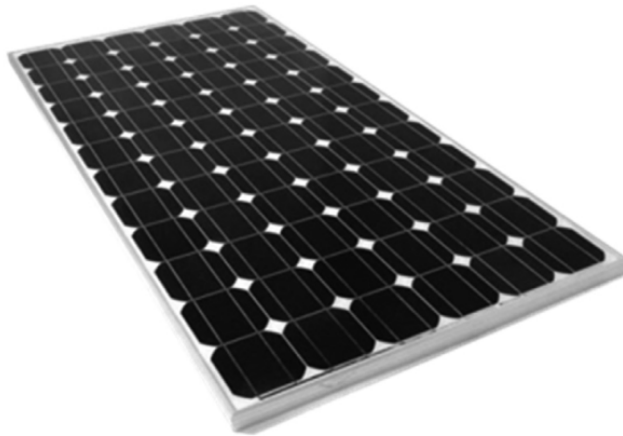


Figure 17 Monocrystalline solar panel [34]

1.8.1.3. Polycrystalline silicon

Cutting a melted and recrystallized silicon ingot produces polycrystalline silicon, also referred to as multicrystalline silicon. Cutting silicon ingots into extremely thin layers and assembling them into solar cells are both steps in the production of polycrystalline solar panels. When compared to monocrystalline cells, this has allowed for a simpler manufacturing process, which in turn has led to cheaper production costs. In a study, Peng et al. [18] used

polycrystalline solar panels to investigate the impact of temperature on the module's efficiency and found that the system may generate a maximum efficiency of more than 7%. The polycrystalline panel in Figure 18 below is created mostly in blue, as opposed to monocrystalline panels, and the cells are often chopped in square or rectangular shapes.

There is also a thick-film variety of polycrystalline panel, which is built of multicrystalline silicon. The cells for this panel are made by continuously depositing silicon on a base material to create a material with a fine grain and lustrous appearance. The efficiency produced by multicrystalline silicon cells is found to be very high and around 20% [19] with today's industrial advances in the engineering of solar panels. The creation of monocrystalline and polycrystalline solar panels is depicted in Figure 18.

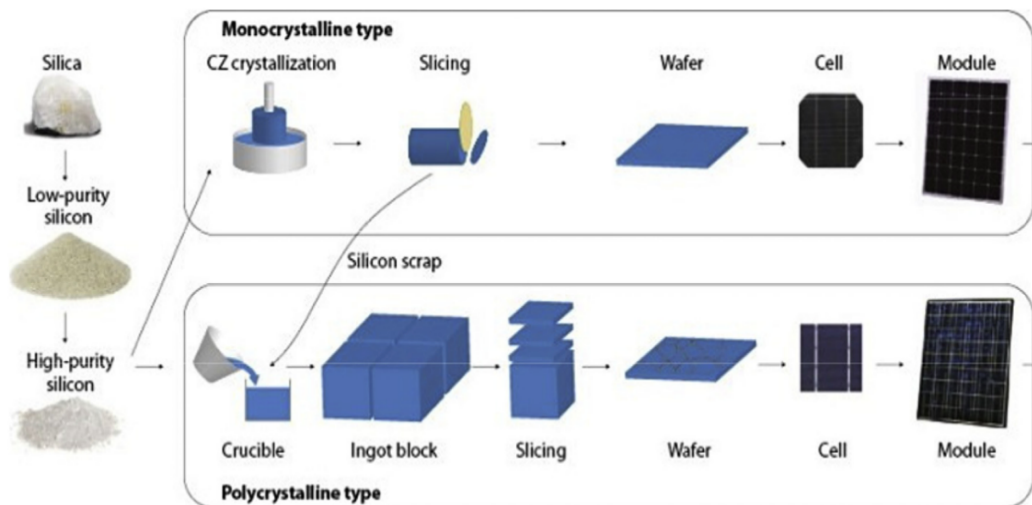


Figure 18 Manufacturing process of mono- and poly-crystalline solar panels [35]

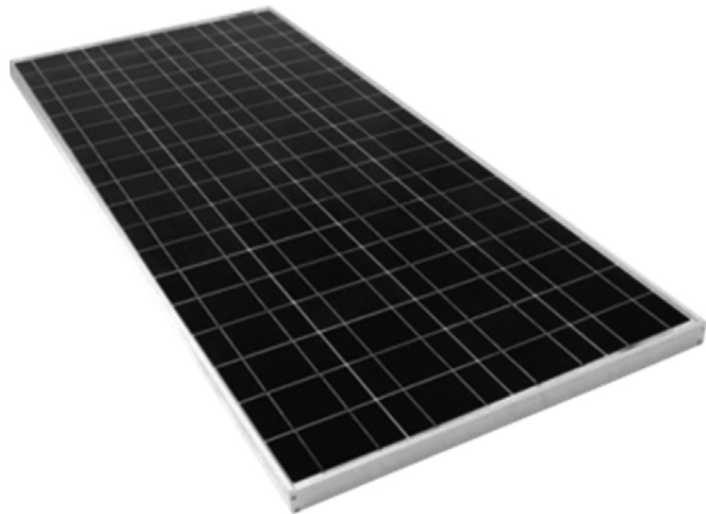


Figure 19 Polycrystalline solar panel [34]

1.8.1.4. Amorphous silicon

Finally, in amorphous silicon, thin homogeneous layers of amorphous silicon are distributed over a surface to produce thin structures, from which the PV cells are made. The PV cells made this way are also referred to as "thin film" since the manufacturing process makes it possible to create incredibly thin and fine layers of silicon. The production of PV panels produced from this silicon may be simpler than with other types of materials because of the properties of amorphous material. Additionally, amorphous silicon may be deposited on both rigid and flexible surfaces, giving rise to the capacity to create variously shaped structures, such as materials for roofs. The efficiency of the cells must be taken into account while designing a panel from this material, even though it can be said that amorphous silicon cells are simpler and less expensive to manufacture [47]. High efficiency amorphous silicon was employed by Wang et al. [21] in an experiment to achieve approximately 12% energy conversion efficiency. The solar panel in Figure 20 below is made of amorphous silicon, which has features that allow it to be flexible and bent in various directions.



Figure 20 Amorphous silicon (thin-film) solar panel [43]

1.8.2. Efficiency of solar panels

Solar panel efficiency varies according to the manufacturing material, size and shape of the cells and the structure of -crystalline. Over the years, studies have observed the growth of efficiency while keeping the other parameters at the optimum level. In Table 2 below, it is clearly seen that as efficiency or the structure of the cell changes, different advantages and disadvantages occur. According to them, choice in terms of purpose of usage might be made.

Table 2 Comparison of different type of solar cells

Advantages and Disadvantages of PV cells.					
Solar Cell	Efficiency Range	Benefits	Drawbacks	Study	Conclusion
Polycrystalline	12-15%	Low price [36]	Sensitive to high temperatures; low lifespan; low efficiency	Impacts of temperature and irradiance on polycrystalline silicon solar cells parameters [39]	The efficiency of the solar cells reduces significantly with an increase in temperature.
Monocrystalline	15-25%	High efficiency; suitable for commercial use; long lifespan [37]	Expensive	Improving spectral modification for applications in solar cells: A review [40]	Monocrystalline solar cells offer a very high output efficiency while are one of the most expensive solar cells in comparison to others.
Amorphous Silicon (Thin-film)	12-15%	Low costs; flexible, easy to fabricate [38]	Short lifespan	A review of thin film solar cell technologies and challenges [41]	The thin-film PV panels offer a short lifespan, however, provide good constructability as being very flexible and lightweight.

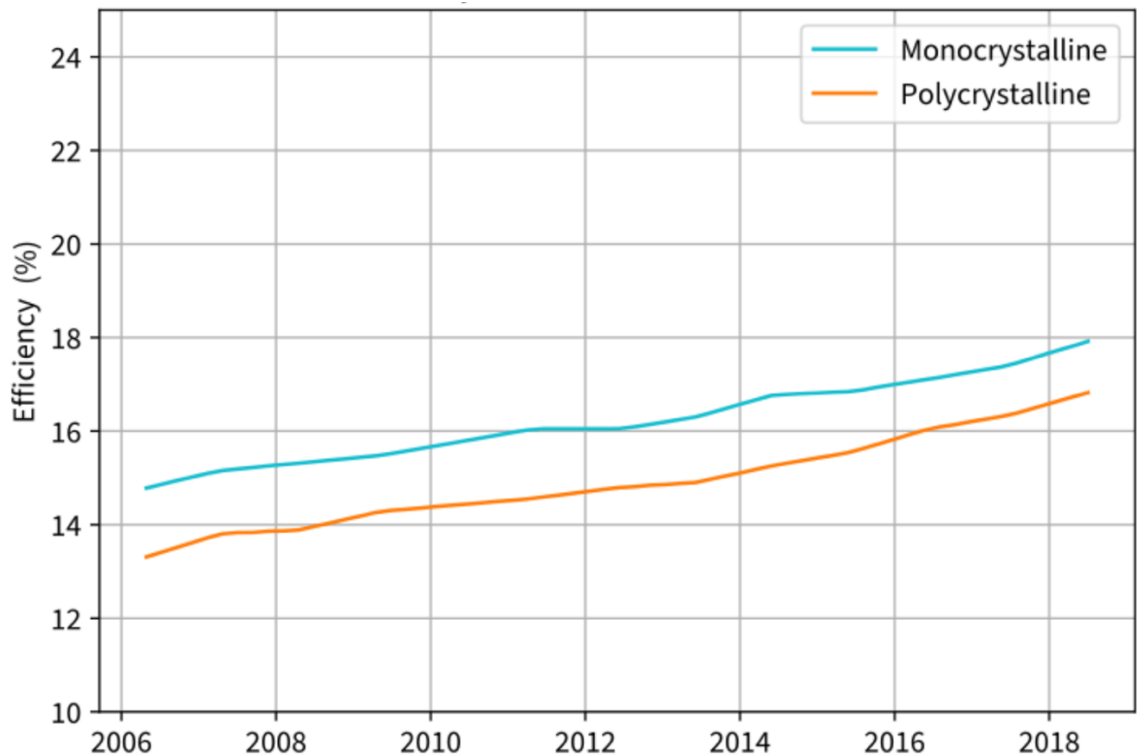


Figure 21 Efficiency of solar panels between 2006-2019 [43]

2. METHODOLOGY

2.1. STIRLING CYCLE CALCULATIONS

There are four different processes in the working principle of Stirling engine as compression, heating, expansion and cooling. In each process, the pressure of the working fluid and the volume of the system change according to the requirement of the current process. Four process is explained below with respect to the Figure 22 and Figure 23.

Table 3 Design parameters and symbols

Parameters	Symbol	Unit
Cold End Temperature (K)	T_c	K
Hot End Temperature (K)	T_h	K
Pressure	$P_1 P_2 P_3 P_4$	kPa
Volume	$V_1 V_2 V_3 V_4$	cm^3
Specific Volume	$v_1 v_2 v_3 v_4$	cm^3
Compression Ratio	RC	-
Specific gas constant	R	kJ/kg-K
Mass of working fluid	m	kg

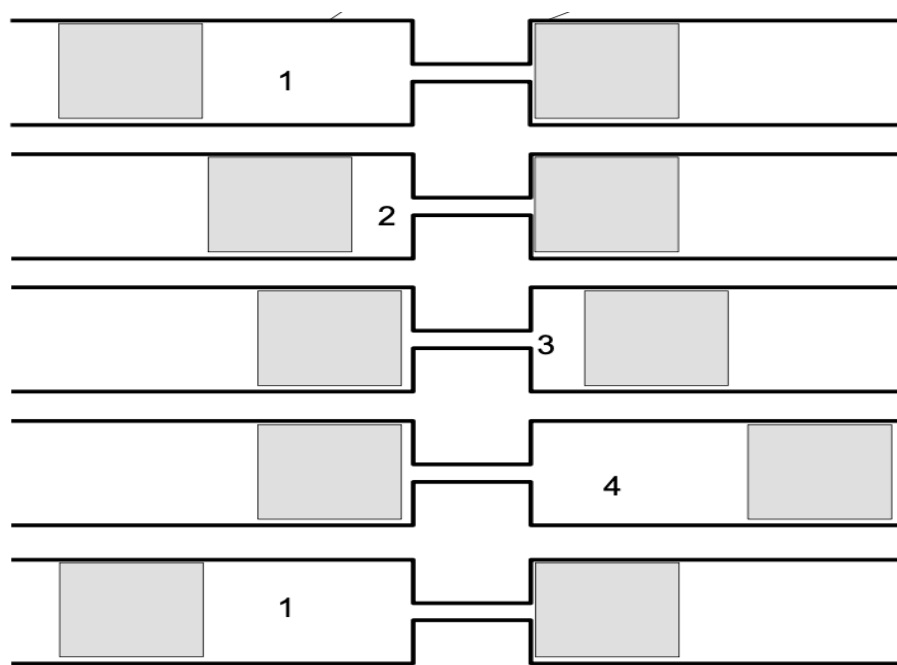


Figure 22 Thermodynamic processes of the Stirling cycle [33]

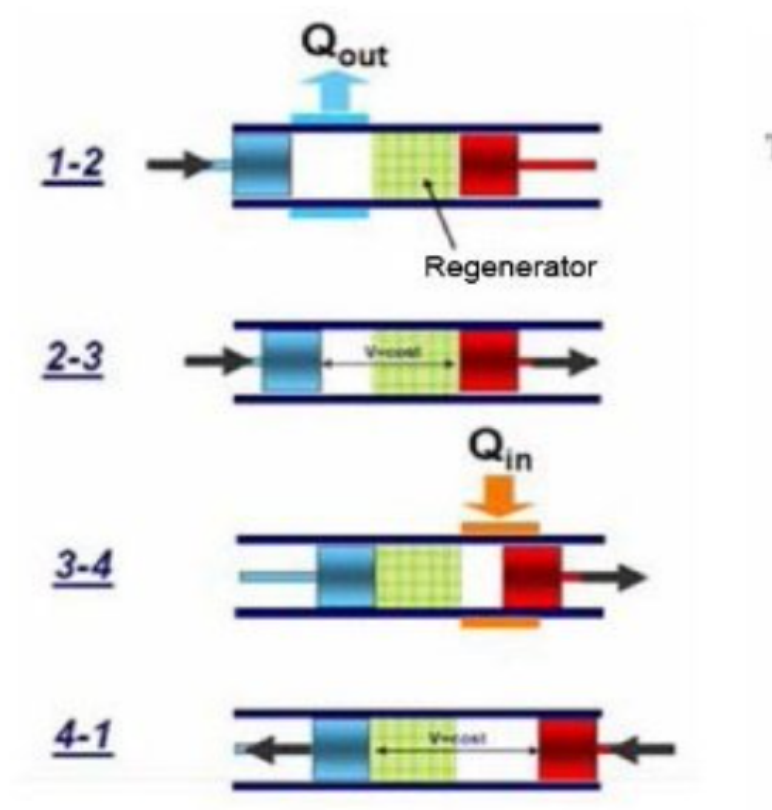


Figure 23 Thermodynamic processes of the cycle [32]

The basic assumptions should be made for the thermodynamic analysis of Stirling cycle,

- Temperature in each gas space (hot and cold) is known and constant.
- Working fluid is assumed to be an Ideal gas.
- There is no leakage into/out of the working fluid.
- There is no friction loss due to the movement of the pistons.

Process 1-2: This process is an isothermal compression process. During this process, compression piston is at the top dead center (TDC). It moves inward and the expansion piston is stationary. When the working fluid is compressed, its pressure increases. The temperature is constant since the heat transferred to the surrounding by the cylinder.

In process 1-2, the cyclic parameters are listed below as,

Pressure:

$$P_1 \quad (2)$$

Volume:

$$V_1 \quad (3)$$

Specific volume:

$$v_1 = \frac{R*T_1}{P_1} \quad (4)$$

Since $T_1=T_c$,

$$v_1 = \frac{R*T_c}{P_1} \quad (5)$$

Temperature:

$$T_1 = T_c \quad (6)$$

The Stirling system releases some heat while the temperature is constant and the compression is on progress. The amount of heat transferred to the surrounding is,

$$Q_{1-2} = m * R * T_1 * \ln\left(\frac{V_1}{V_2}\right) \quad (7)$$

Since $T_1=T_c$, the equation becomes,

$$Q_{1-2} = m * R * T_c * \ln\left(\frac{V_1}{V_2}\right) \quad (8)$$

where mass of working fluid is equal to,

$$m = \frac{P_1 * V_1}{R * T_c} \quad (9)$$

Process 2-3: At this stage, both piston moves accordingly. While working piston keeps moving towards regenerator, expansion piston gets away from the regenerator. After the working fluid passes through the regenerator, it starts to expand. The regenerator provides the working fluid with pre-heating. At the same time, increase in pressure occurs.

Pressure:

$$P_2 = P_1 * \frac{V_1}{V_2} \quad (10)$$

Volume:

$$V_2 = \frac{V_1}{R C} \quad (11)$$

Specific volume:

$$v_2 = \frac{R * T_c * V_2}{V_1 * P_1} \quad (12)$$

Temperature:

$$T_2 = T_c \quad (13)$$

Since the regenerator has an active role with pre-heating the working fluid, there is an amount of heat stored in regenerator which is calculated as,

$$Q_{2-3} = m * c_v * (1 - E_c) * (T_3 - T_2) \quad (14)$$

Since $T_2 = T_h$ and $T_3 = T_c$,

$$Q_{2-3} = m * c_v * (1 - E_c) * (T_h - T_c) \quad (15)$$

Where E_c is the effectiveness for cold sides of regenerator,

$$E_c = \frac{T_H - T_{1'}}{T_H - T_C} \quad (16)$$

Thus,

$$T_{1'} = T_H - E_c(T_H - T_C) \quad (17)$$

Process 3-4: Expansion process is fulfilled in this process. The piston which is working in the hot side of the cylinder moves towards TDC and the compression piston is stationary at the bottom dead center (BDC). During expansion, the volume of the system increases and accordingly the pressure decreases. However, the temperature stays constant because the heat is transferred to the system from an external source.

Pressure:

$$P_3 = P_1 * \frac{V_1}{V_2} * \frac{T_h}{T_c} \quad (18)$$

Volume:

$$V_3 = V_2 = \frac{V_1}{Rc} \quad (19)$$

Specific volume:

$$v_3 = v_2 = \frac{R*T_c*V_2}{V_1*P_1} \quad (20)$$

Temperature:

$$T_3 = T_h \quad (21)$$

The amount of heat that should be applied to the system by solar radiation,

$$Q_{3-4} = m * R * T_3 * \ln\left(\frac{V_4}{V_3}\right) \quad (22)$$

Since $T_3 = T_h$ and $V_3 = V_2$ and $V_4 = V_1$,

$$Q_{3-4} = m * R * T_h * \ln\left(\frac{V_1}{V_2}\right) \quad (23)$$

Process 4-1: This process is the last process of the working principle for Stirling engine. Likewise, the process 2-3, both pistons move at the same time. The working fluid is transferred to the starting position at the constant volume. During this step, it starts compression from expansion. In the regenerator, the heat is transferred to the fluid from the regenerator. The temperature of the working fluid keeps decreasing. The heat transferred to the regenerator is used in process 2-3 at the next cycle.

Pressure:

$$P_2 = P_1 * \frac{V_1}{V_2} \quad (24)$$

Volume:

$$V_4 = V_1 \quad (25)$$

Specific volume:

$$v_4 = v_1 \quad (26)$$

Temperature:

$$T_4 = T_h \quad (27)$$

The amount of heat applied to the system from the regenerator,

$$Q_{4-1} = m * c_v * (1 - E_H) * (T_4 - T_1) \quad (28)$$

Since $T_4 = T_h$ and $T_1 = T_c$,

$$Q_{4-1} = m * c_v * (1 - E_H) * (T_h - T_c) \quad (29)$$

Where E_H is the effectiveness for hot sides of regenerator,

$$E_H = \frac{T_{3'} - T_2}{T_3 - T_2} = \frac{T_{3'} - T_c}{T_h - T_c} \quad (30)$$

Thus,

$$T_{3'} = T_C + E_H(T_H - T_C) \quad (31)$$

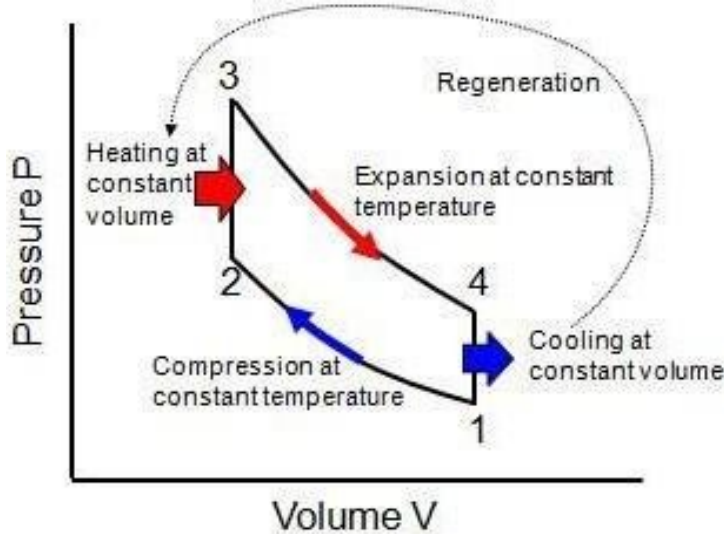


Figure 24 P-v diagram of the Stirling Engine

As it discussed in previous processes, if we consider $Q_{2-3}=Q_{4-1}$, the regenerator must have the same effectiveness in cold and hot sides which means,

$$E_H = E_C = E \quad (32)$$

Therefore, the estimation of the regenerator effective temperature is important. Three main approaches for estimation of regenerator effective temperature (T_R) are as follows.

[Asnaghi,27]

(i) Arithmetic mean approach:

$$T_R = \frac{T_{1'} + T_{3'}}{2} \quad (33)$$

(ii) Logarithmic mean approach:

$$T_R = \frac{T_{3'} - T_{1'}}{\ln(T_{3'}/T_{1'})} \quad (34)$$

(iii) Half hot space – half cold space approach:

$$\frac{1}{T_R} = \frac{1}{2} \left(\frac{1}{T_1} + \frac{1}{T_3} \right) \quad (35)$$

By substituting (17) and (31) with (33),

$$T_R = \frac{T_H + T_C}{2} \quad (36)$$

As it is clear in (36), in the arithmetic mean approach the regenerator effective temperature is not depended on the effectiveness of the regenerator. However, in the two other approaches, the effective temperature of regenerator is dependent on the regenerator effectiveness. [27]

The amount of heat supplied (Q_s) to the system can be calculated as,

$$Q_s = Q_{2-3} + Q_{3-4} \quad (37)$$

The amount of heat released (Q_r) during the cycle is,

$$Q_r = Q_{1-2} + Q_{4-1} \quad (38)$$

The net amount of heat (Q_{net}) is calculated with respect to Q_s and Q_r ,

$$Q_{net} = Q_s - Q_r \quad (39)$$

Which is also equal to,

$$Q_{net} = (T_h - T_c) * R * \ln\left(\frac{V_1}{V_2}\right) \quad (40)$$

According to the calculations made in previous steps, the Stirling efficiency (η_s) can be calculated by the formula of,

$$\eta_s = \frac{Q_{net}}{Q_s} = \frac{(T_h - T_c) * R * \ln\left(\frac{V_1}{V_2}\right)}{C_v * (1-E) * (T_h - T_c) + R * T_h * \ln\left(\frac{V_1}{V_2}\right)} \quad (41)$$

2.2. Solar Radiation Calculations

The solar energy that comes per second to an area of 1 m^2 perpendicular to the sun's rays is 1367 J. This number is called the "Solar Constant – I_{sc} ". The solar constant is 1367 W/m^2 . On Earth, the most important characteristics of radiation are determined by the Earth's rotation around its axis and its elliptical orbit around the Sun. Specific angles are formed between the rays coming from the Sun and the surfaces on Earth. To effectively utilize solar energy, knowledge of solar angles is necessary.

2.2.1. Latitude Angle (ϕ)

The angle between the line connecting any point on the Earth's surface to the center of the Earth and the Earth's equatorial plane is called the latitude. It varies between -90° and 90° , with the north direction being positive ($-90^\circ \leq \phi \leq 90^\circ$). The latitude angle can be read from an atlas for any given region. Turkey is located between $36-42^\circ$ north latitudes ($26^\circ-45^\circ$ east longitudes). The latitude angle is also used in calculating the solar altitude angle.

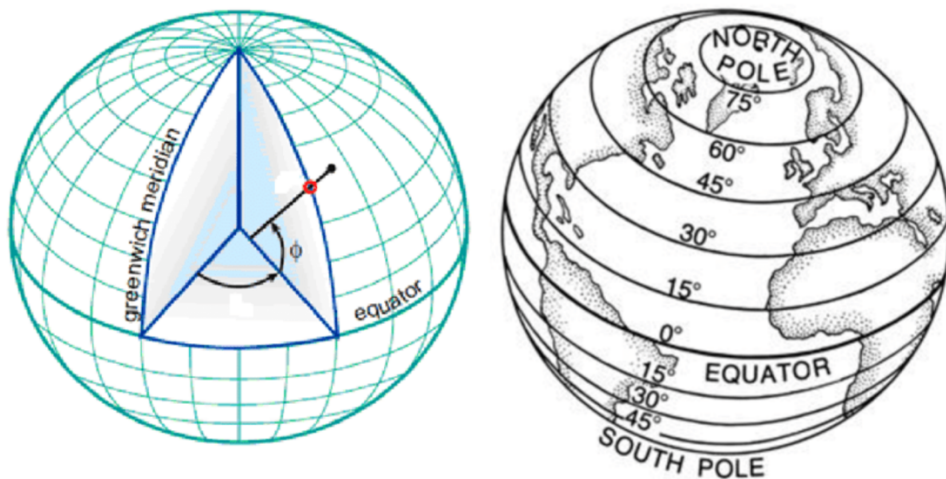


Figure 25 Scheme of latitude [31]

2.2.2. Declination Angle (δ)

The angle between the sun's beams and the equatorial plane, which varies with the months and seasons, is also known as the angle at which solar rays strike Earth. It is also known by the name declination angle. The Earth's own axis's 23.45-degree angle with its orbital plane is what determines the declination angle. (The declination angle would always be 'zero' if the Earth's axis of rotation were not slanted.) The Earth's polar axis, which is fixed in space at an

angle of 66.55° to its orbital plane, explains why the declination angle lies within this range of -23.45° to 23.45° . For clarification, the angle between the orbital plane and the equatorial plane of the Earth is at its maximum (23.45°) on June 21 and its minimum (-23.45°) on December 21. The declination angle is 'zero' at the equinox points, which are March 21 for the vernal equinox and September 22 for the autumnal equinox.

Determining the approximate declination angle using three alternative formulas,

$$\delta = -23.45 \cos \left[\frac{360}{365} (10 + d) \right] \quad (42)$$

$$\delta = 23.45 \sin \left[\frac{360}{365} (284 + d) \right] \quad (43)$$

$$\delta = 23.45 \sin \left[\frac{360}{365} (d - 81) \right] \quad (44)$$

where d is the day number of the year.

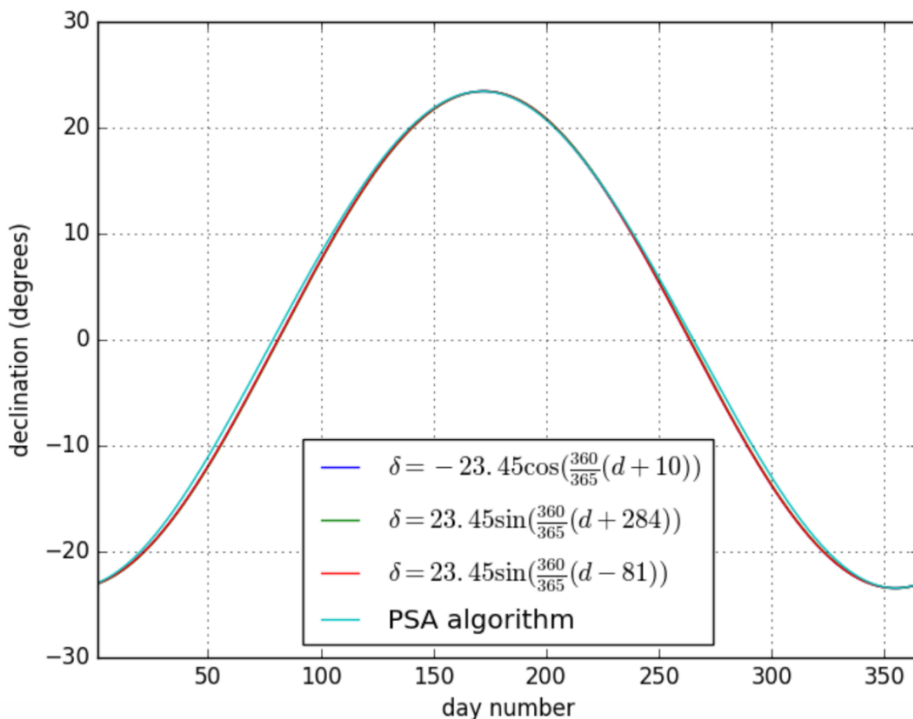


Figure 26 Declination angle vs. day number graph with three formulas

2.2.3. Hour Angle (ω)

The angle formed by the solar longitude—also referred to as solar longitude—and the longitude of the site being seen is known as the solar azimuth angle. Before and after the solar longitude crosses with the longitude of the observed site at "solar noon," the hour angle is

calculated as (-) and (+), respectively. The solar hour is 12 at solar noon. The solar hour angle is calculated by adding a constant factor of 15 to the time difference between solar noon and the provided time. The 360° angle that the Earth makes in one rotation around the Sun is divided by 24 to get this constant factor. In other words, the angle that the Earth makes around the Sun in each hour is represented by this coefficient. One hour corresponds to 15 degrees of longitude. Solar angles are symmetrical with respect to solar noon.

The formula of hour angle is,

$$\omega = 15 * (\text{SH} - 12) \quad (45)$$

where SH is solar hour.

2.2.4. Solar Elevation(Altitude) Angle (α)

The solar elevation(altitude) angle is the angle between the direct solar ray and the horizontal plane. In every season, the solar altitude angle is highest at noon, and it is zero at sunrise and dusk. On December 21st, the solar altitude angle is at its lowest point, while on June 21st, it is at its highest point.

$$\alpha = \sin^{-1}(\sin(\varphi) \sin(\delta) + \cos(\delta) \cos(\omega) \cos(\varphi)) \quad (46)$$

Since the solar altitude angle completes the zenith angle to 90° degrees, the formula can be written also as,

$$\alpha = 90 - \psi \quad (47)$$

2.2.5. Zenith Angle (ψ)

The angle formed by the direct sun radiation and the vertical plane is known as the zenith angle. In other terms, the zenith angle is the angle at which the sun rays cross the horizontal plane. When the solar beams are perpendicular, the zenith angle is zero, but it is 90° at sunrise and sunset.

It can be found with the formula of,

$$\cos(\psi) = \sin(\varphi) \sin(\delta) + \cos(\delta) \cos(\omega) \cos(\varphi) \quad (48)$$

2.2.6.Solar Azimuth Angle (γ_s)

The angle formed by the projection of the sun direction on a horizontal plane and the north-south direction is known as the solar azimuth angle. It represents the angle formed by the direct sun radiation and the north-south axis. Additionally, the solar azimuth angle shows the deviation from the north in a clockwise orientation. In terms of the east and west, it is regarded as negative (-) and positive (+), respectively. The azimuth angle is 180 degrees at 12:00. The surface-solar azimuth angle is the angle formed by direct radiation and the perpendicular surface. The formula of solar azimuth angle is given below as,

$$\sin(\gamma) = -\frac{\cos(\delta) \sin(\omega)}{\sin(\psi)} \quad (49)$$

or

$$\gamma = \sin^{-1} \left(-\frac{\cos(\delta) \sin(\omega)}{\sin(\psi)} \right) \quad (50)$$

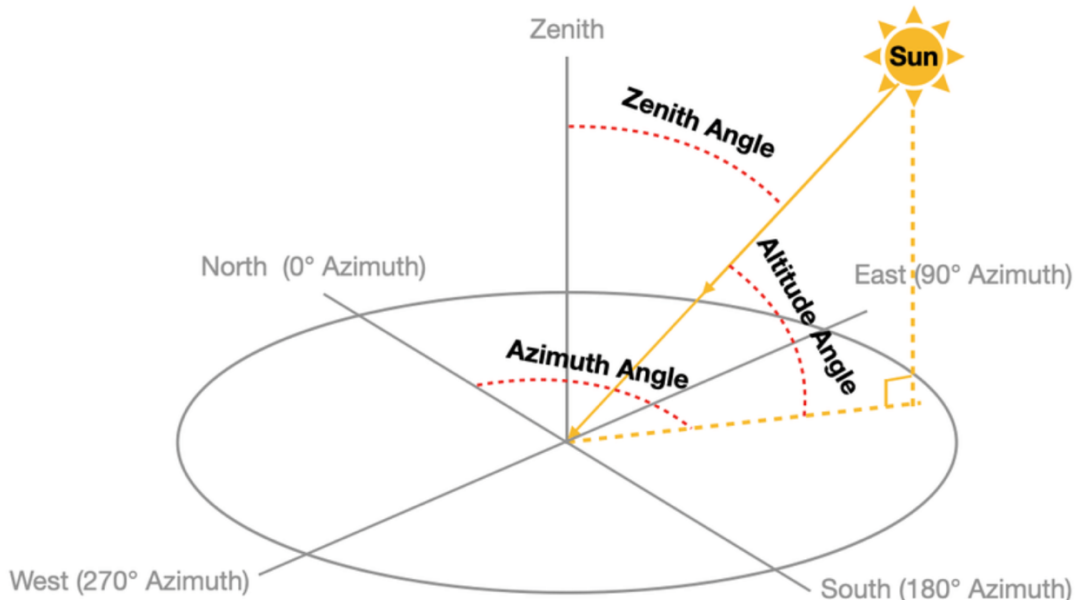


Figure 27 Illustration of zenith, altitude and azimuth angle [30]

2.2.7.Solar Radiation

Extraterrestrial solar radiation is the radiation that in the absence of an atmosphere, strikes the earth's surface. It is the solar radiation that reaches the earth's surface through the open atmosphere. Without the influence of the atmosphere, it can be calculated.

Terrestrial solar radiation is solar energy that hits the earth's surface while the atmosphere is still in place. Depending on the climate and the condition of the sky, it can alter. From the database, it can be measured or estimated.

The formula for two radiation type is,

$$I_0 = \frac{24*3600*I_{sc}}{\pi} \left[1 + 0.033 \cos\left(\frac{360n}{365}\right) \right] * \left[\cos \varphi \cos \delta \sin \omega + \frac{\pi \omega}{180} \sin \varphi \sin \delta \right] \quad (51)$$

Also, to calculate it over a certain time,

$$I_0 = \frac{24*3600*I_{sc}}{\pi} \left[1 + 0.033 \cos\left(\frac{360n}{365}\right) \right] * \left[\cos \varphi \cos \delta (\sin \omega_2 - \sin \omega_1) + \frac{\pi(\omega_2 - \omega_1)}{180} \sin \varphi \sin \delta \right] \quad (52)$$

where the unit of I_0 is MJ/m²-day.

ÇİZELGE III.1 Yeryüzünde Yatay Düzleme Gelen (YYRA) ve Atmosfer Üçnisi (AÖRA) Aylık Ortalama Radyasyon Değerleri (Kcal/m ² /gün)												
	Ocak	Şubat	Mart	Nisan	Mayıs	Hazır	Temmuz	Ağustos	Eylül	Ekim	Kasım	Aralı
Adana E=36.5	1792 4087	2533 5306	3394 6859	4278 8389	5162 9440	5245 8947	5138 9632	4660 8771	4684 7385	2987 5760	2103 4374	1697 3752
Adiyaman E=37.4	1649 3967	2270 5210	3322 6764	4445 8341	5592 9440	6500 9871	6477 9632	5855 8747	4660 7313	3250 5640	2031 4254	1553 3633
Ankara E=39.6	1266 3657	2007 4923	3035 6547	4138 8222	5258 9393	5855 9871	6094 9632	5425 8652	4278 7146	2916 5377	1816 3943	1051 3322
Afyon E=38.4	1410 3826	2247 5067	3179 6644	4254 8293	5306 9417	5808 9871	6047 9632	5401 8700	4278 7242	2916 5521	2032 4111	1315 3489
Antalya E=39.4	1864 4111	2557 5330	3489 6859	4445 8389	5283 9440	5688 9847	5521 9632	4995 8795	4182 7409	3059 7409	2223 5760	1697 4374
Balıkesir E=39.4	1267 3681	1936 4947	2820 6547	3967 8222	5234 9393	5760 9871	5784 9632	5186 8676	4063 7146	2653 5401	1673 5401	1147 3346
Bilecik E=37.0	1673 4039	2342 5258	3394 6811	4589 8365	5664 9440	6333 9847	6238 9632	5616 8771	4589 7361	3203 5712	2103 4302	1527 3681
Bolu E=40.4	1171 3537	1888 4804	2844 6453	3824 8174	4756 9393	5306 9871	5306 9628	4684 8628	3800 7050	2487 5282	1601 3824	1099 3179
Burdur E=37.4	1625 3967	2414 5210	3370 6764	4302 8341	5545 9440	5951 9871	6190 9632	5569 8747	4421 7313	3059 5640	2079 4254	1458 3933
Bursa E=40.1	1243 3585	1912 4852	2677 6477	3776 8174	4995 9393	5497 9871	5545 9608	4876 8628	3824 7074	2533 5306	1649 3872	1195 3226
Canakkale E=40.1	1290 3585	2055 4852	2987 6477	4230 8198	5377 9393	5712 9871	5784 9608	5090 8628	3943 7098	2605 5328	1721 3872	1243 3250
Cankiri E=39.4	1075 3537	1768 4804	2892 6572	3872 8174	4699 9393	5473 9871	5616 9608	4876 8628	3872 7050	2653 5282	1553 3848	908 3203

ÇİZELGE III.1 (devam)												
	Ocak	Şubat	Mart	Nisan	Mayıs	Hazır	Temmuz	Ağustos	Eylül	Ekim	Kasım	Aralı
Denizli E=37.5	1625 3957	2342 5186	3226 6764	4158 8341	5401 9440	5927 9871	5927 9632	5353 8747	4350 7313	2963 5640	2007 4254	1462 3633
Elazığ E=38.4	1243 3824	1936 5067	3155 6668	4278 8293	5497 9417	6333 9871	6381 9632	5688 8700	4517 7242	2963 5521	1673 4111	1075 3489
Erzincan E=39.6	1362 3661	2302 4923	3167 6549	3991 8222	5057 9393	5855 9871	6070 9632	5611 8676	4230 7146	2844 5401	1745 3967	1195 3346
Erzurum E=39.6	1434 3657	2223 4923	3131 6549	4182 8222	5067 9393	5808 9871	5827 9632	5306 8652	4206 7146	2916 5377	1768 3943	1314 3322
Eskişehir E=39.5	1219 3681	1960 4923	2987 6549	3919 8222	5138 9393	5712 9871	5903 9632	5213 8677	4182 7146	2700 5401	1673 3967	1027 3322
Gaziantep E=37.1	1673 4015	2318 5258	3346 6811	4517 8365	5640 9440	6333 9847	6238 9632	5497 8771	4445 7361	3226 5688	2127 4302	1577 3681
İsparta E=37.4	1625 3967	2366 5210	3322 6764	4254 8341	5354 9440	5903 9871	6094 9632	5449 8747	4493 7313	2987 5640	2055 4254	1506 3633
İstanbul E=41.0	1099 3442	1792 4732	2629 6381	3943 8126	4947 9369	5401 9871	5186 9608	4613 8604	3561 7003	2414 5210	1482 3752	1677 3107
İzmir E=38.2	1625 3848	2342 5091	3322 6668	4350 8293	5449 9417	5712 9871	5760 9632	5330 8723	4302 7242	2964 5545	1912 4135	1458 3513
İzmit E=40.5	1123 3537	1793 4804	2510 6429	3585 8150	4684 9393	5115 9871	5043 9608	4445 8628	3442 7051	2223 5282	1482 3824	1052 3179
Kars E=40.4	1315 3537	2055 4804	2988 6453	3991 8173	4708 9393	5593 9871	5664 9608	5067 8628	3991 7051	2820 5282	1697 3848	1119 3203
Kastamonu E=41.2	1147 3418	1864 4684	3019 6357	3846 8102	4804 9369	5354 9871	5521 9608	4923 8580	3824 6979	2510 5162	1530 3705	932 3083

Figure 28 The comparison of process of solar radiations

The chart given above (Figure 28) provides information about the comparison of the average solar radiation before atmosphere and average solar radiation on horizontal plane, on earth. In Istanbul, it illustrates that the loss due to the atmosphere effects in January is 2343 kcal/m²-day which is roughly (1 kcal = 4.18 kJ) equal to 9794 kJ/m²-day. The rate of loss is about 68% while it drops to 48% in June and 60.5% in November. While terrestrial solar radiation is calculated, the atmosphere effects have to take into consideration.

3. RESULTS

3.1. Simulation application on MATLAB software

In this study, a simulation program to investigate the parameters was created by MATLAB software shown in Figure 29. The inputs are on the left side, so the user can enter an input to go into details about that parameter specifically. With the drop-down menu, the gas type can be chosen to see the effects of gasses to the system. Besides these inputs of Stirling cycle, solar month can be chosen to compare the solar radiation on that month or day.

With respect to the selected input parameters, graphs are plotted in the Figure 30. Result will vary with different gasses. The graph that illustrates the comparison of all the gasses at the same will be given in the following.

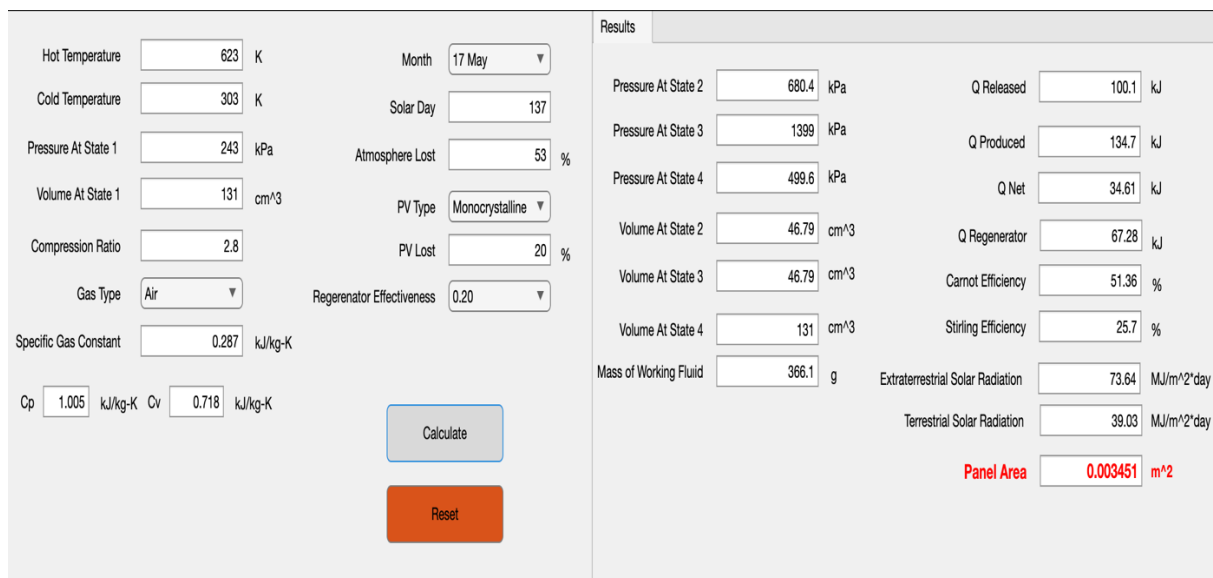


Figure 29 The interface of the simulation application on MATLAB

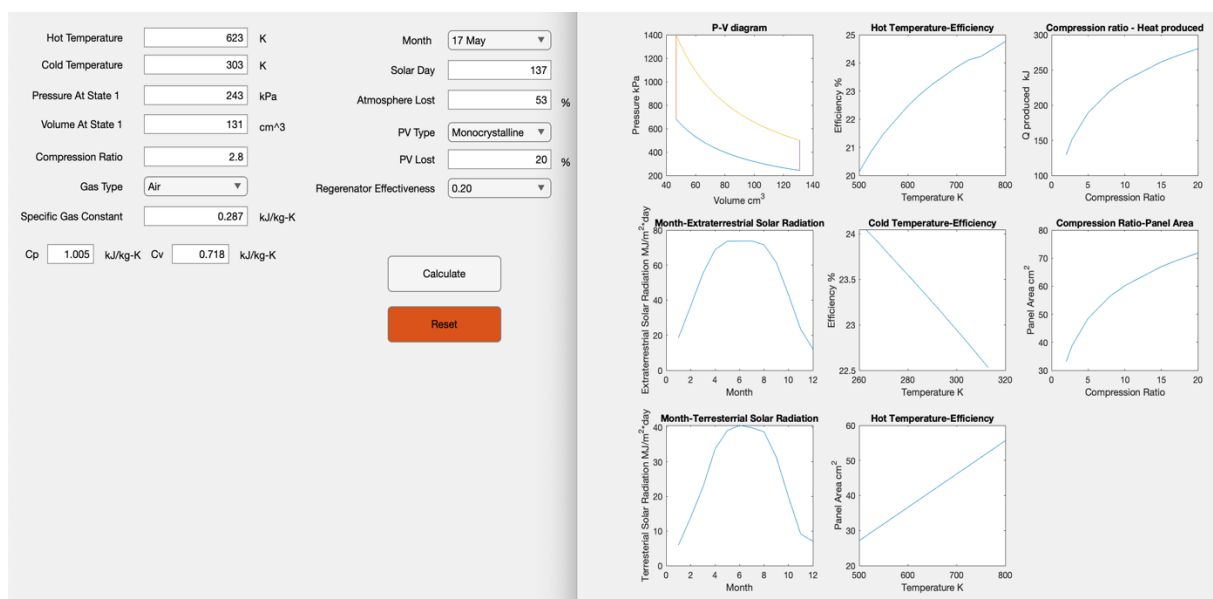


Figure 30 Outputs of the application

This picture is known as the work diagram because the integration of the area within the P-V curve displays the net work. The locations of points 3 and 4 in the P-V diagram (Figure 31) of the Stirling engine are theoretically indicated by the hot temperature. Increased high temperature causes these two sites' pressure to rise when their volume and mass are both constant. At the state 3, pressure has its maximum value of 1399 kPa while the volume reaches its lowest point which is about 47 cm³. The pressure is 243 kPa at state 1, when the piston gets started the compression process with constant temperature of 303 K and the volume of 131 cm³.

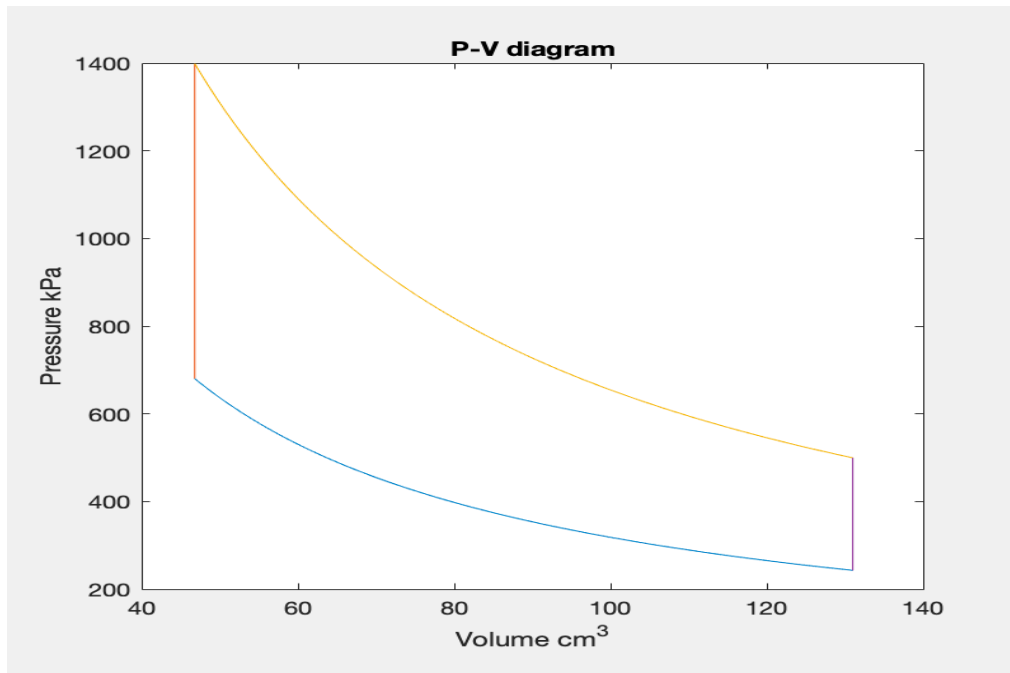


Figure 31 P-V diagram of Stirling cycle

3.2. Effects of hot and cold temperature on efficiency with Stirling and Carnot cycle

When investigating the variations of efficiency with respect to hot temperature and cold temperature in terms of Stirling and Carnot cycles. As hot temperature increases, efficiency shows an upward trend continuously. Although Stirling cycle efficiency illustrates the same manner, its rise is roughly 5% beginning from 500 K to 800 K. Also, it reaches approximately its steady value as hot temperature increases. On the other hand, the minimum efficiency of

Stirling and Carnot cycle is 20% and 40%, respectively.

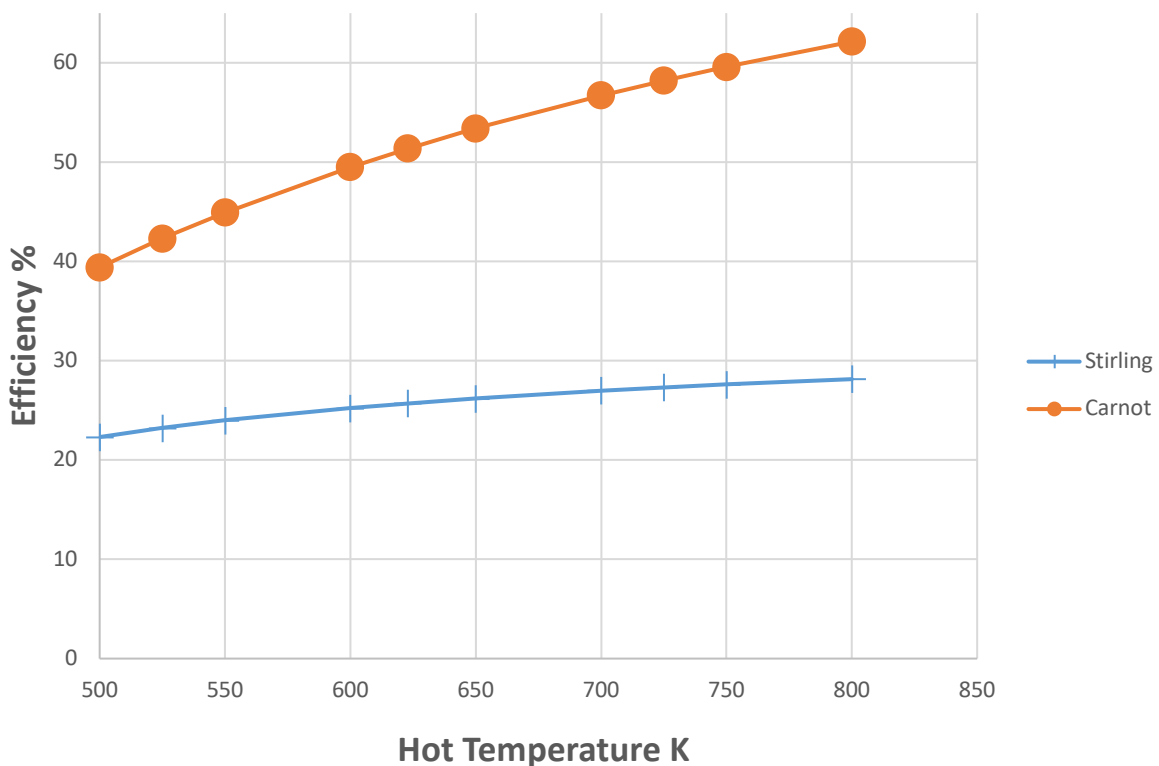


Figure 32 The variations of total input heat against hot temperature for different working gas

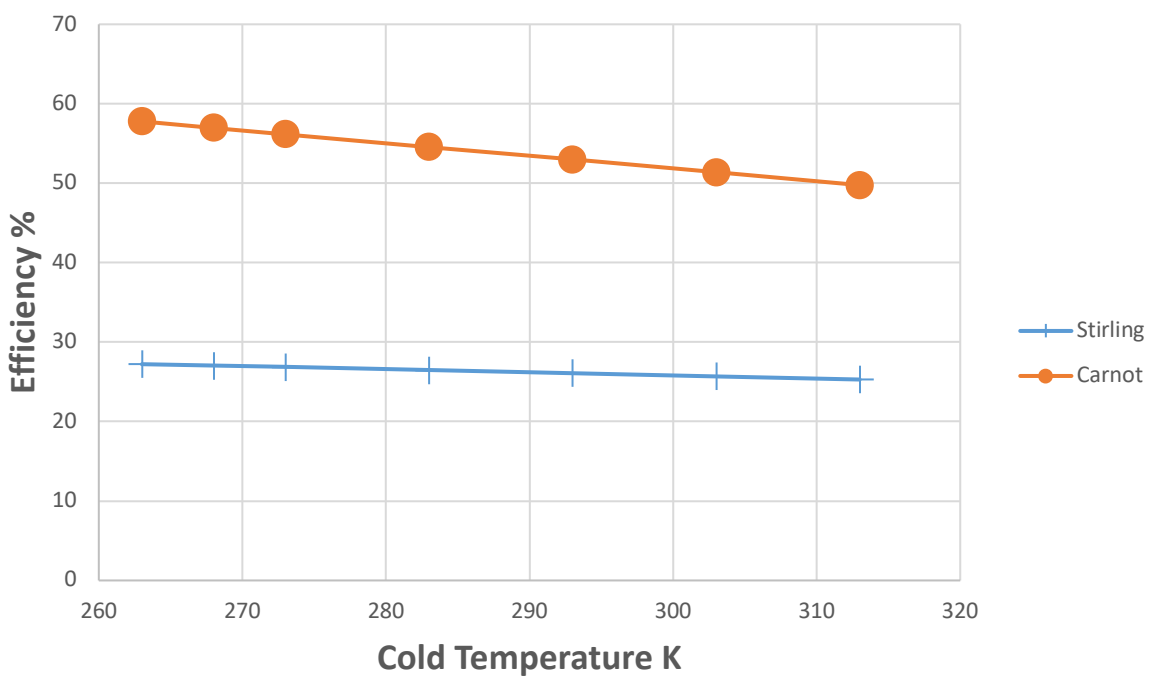


Figure 33 The variations of total input heat against cold temperature for different working gas types.

3.3. Effects of hot temperature on different gasses

An increase in heat will cause both net work and total input heat to increase. An rise in hot temperature has more effects on net work than total input heat, which will boost thermal efficiency, when the gap between hot temperature and cold temperature is small, hot temperature from 500 to 800K in Figure 34. The increasing rate in net work and total input heat are almost equivalent at higher hot temperature values, hot temperature greater than 600 K in Figure 34, and as a result, thermal efficiency tends to a limiting value in Figure 35.

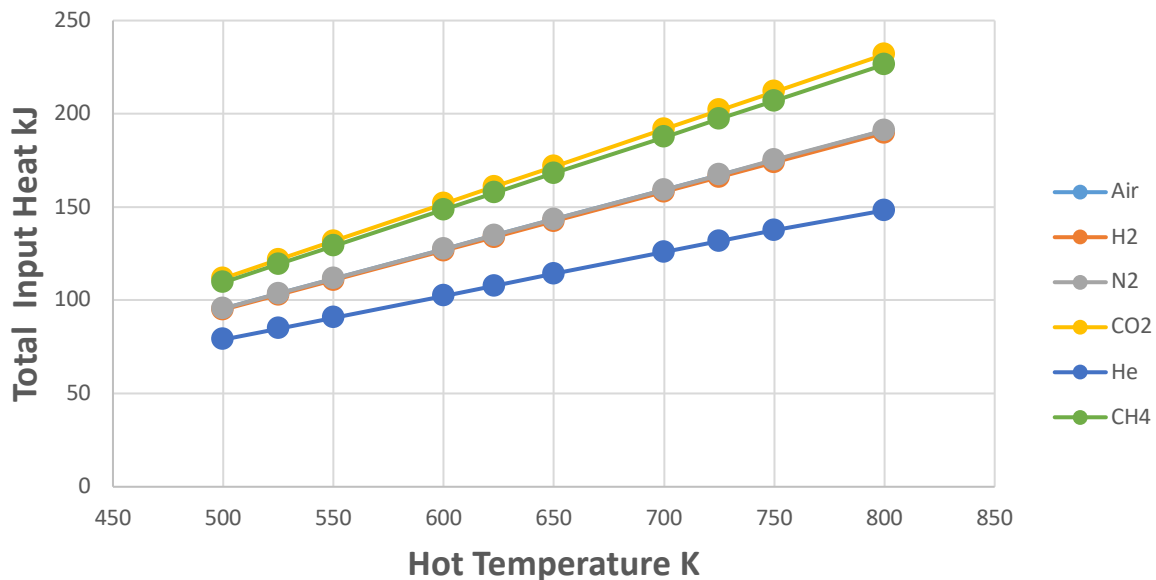


Figure 34 The variations of total input heat against hot temperature for different gasses

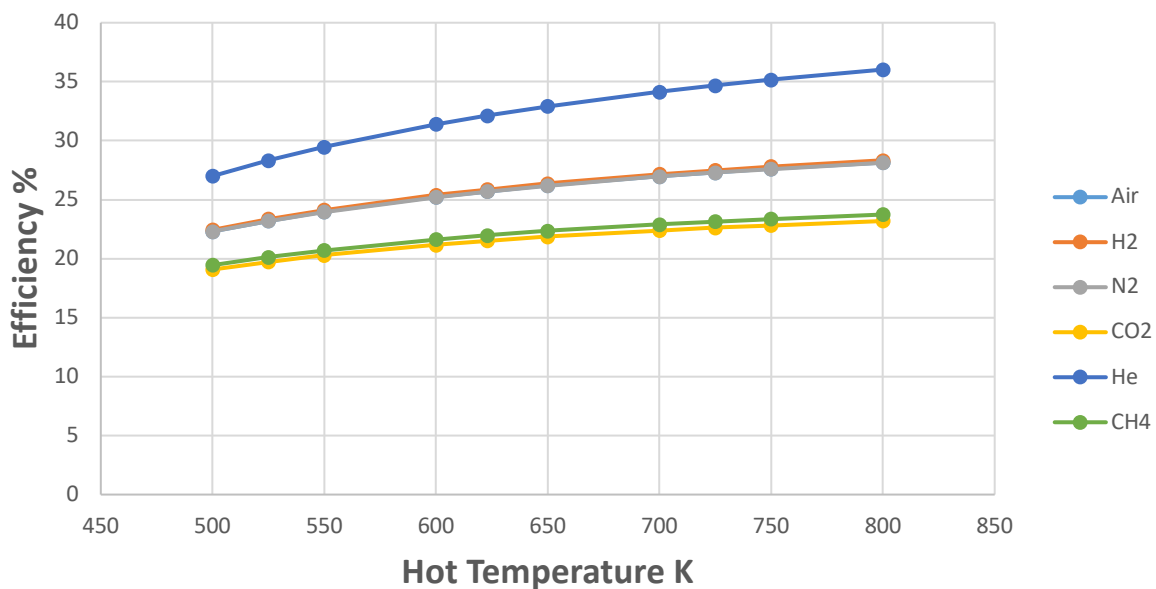


Figure 35 The variations of efficiency against hot temperature for different gasses

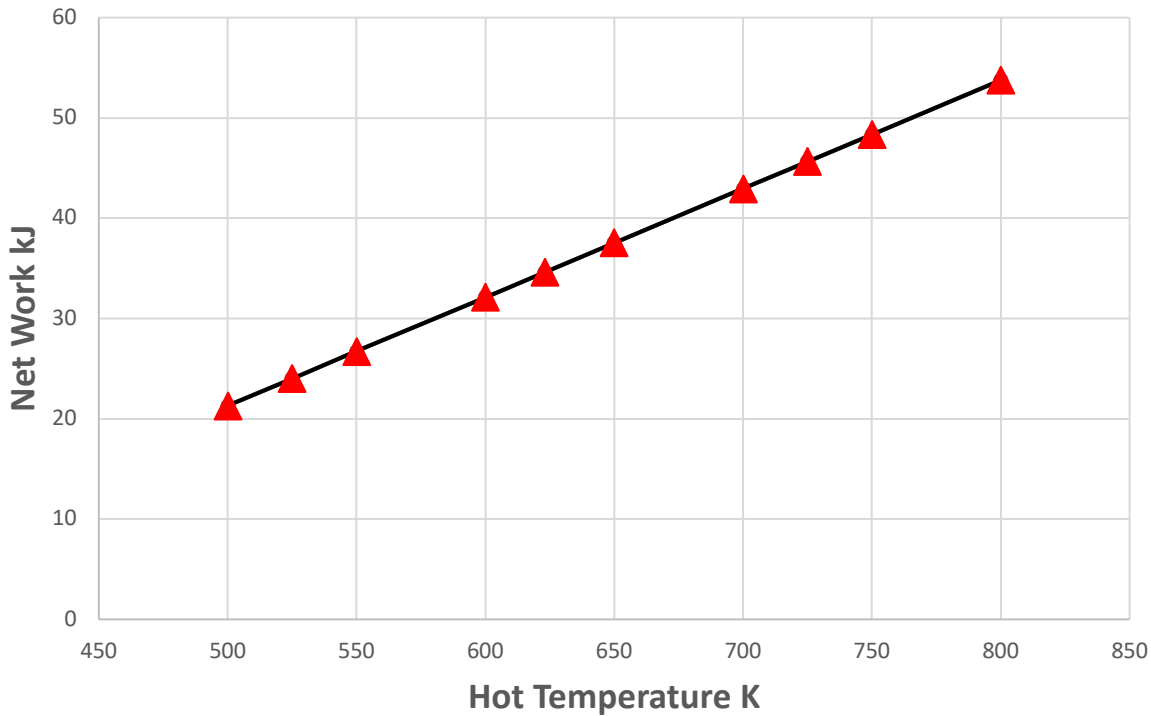


Figure 36 The variations of net work against hot temperature

3.4. The effects of regenerator effectiveness with hot temperature variations

With different regenerator effectiveness, total heat input varies according to the hot temperature. As it is seen in Figure 37, as regenerator effectiveness getting higher, the total input heat at the constant hot temperature decreases. With comparison of E=0.4 and E=0.6 at 750 K, the amount of total input heat was about 150 kJ with the effectiveness of 0.4 while it is roughly 125 kJ with the effectiveness of 0.6.

On the other hand, the opposite situation occurs for the variation of efficiency with respect to the regenerator effectiveness. At constant hot temperature, as regenerator effectiveness increases the Stirling efficiency rises, proportionally. At 500 K, the efficiency is approximately 21% and 32% when the effectiveness is 0.2 and 0.8, respectively.

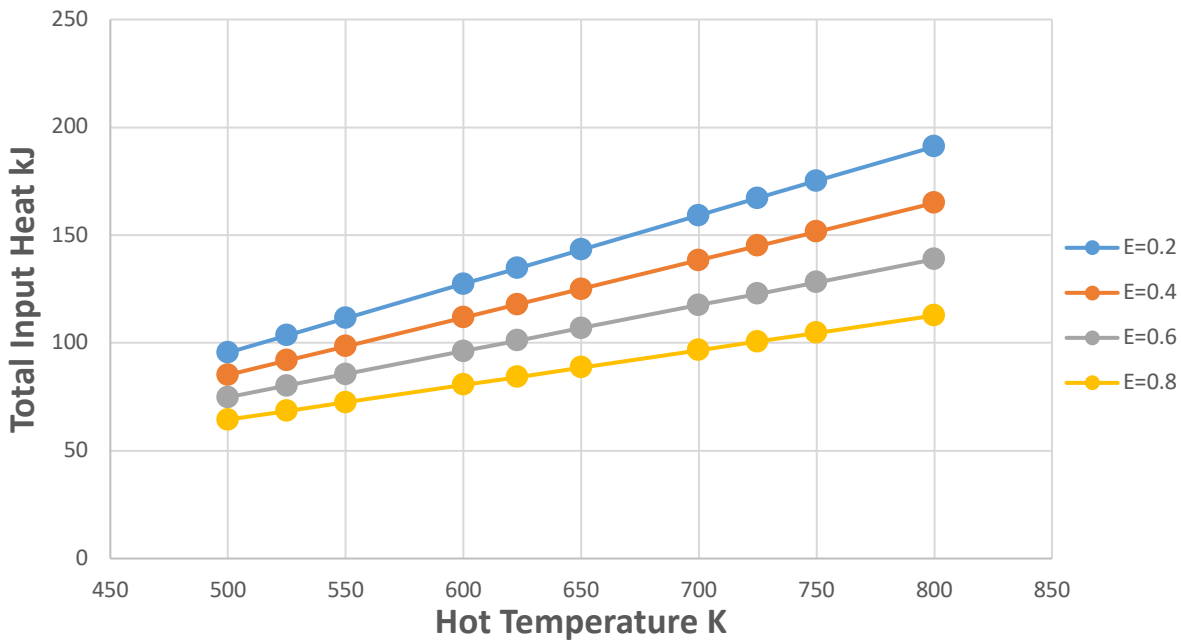


Figure 37 The variations of total input heat against hot temperature for regenerator effectiveness

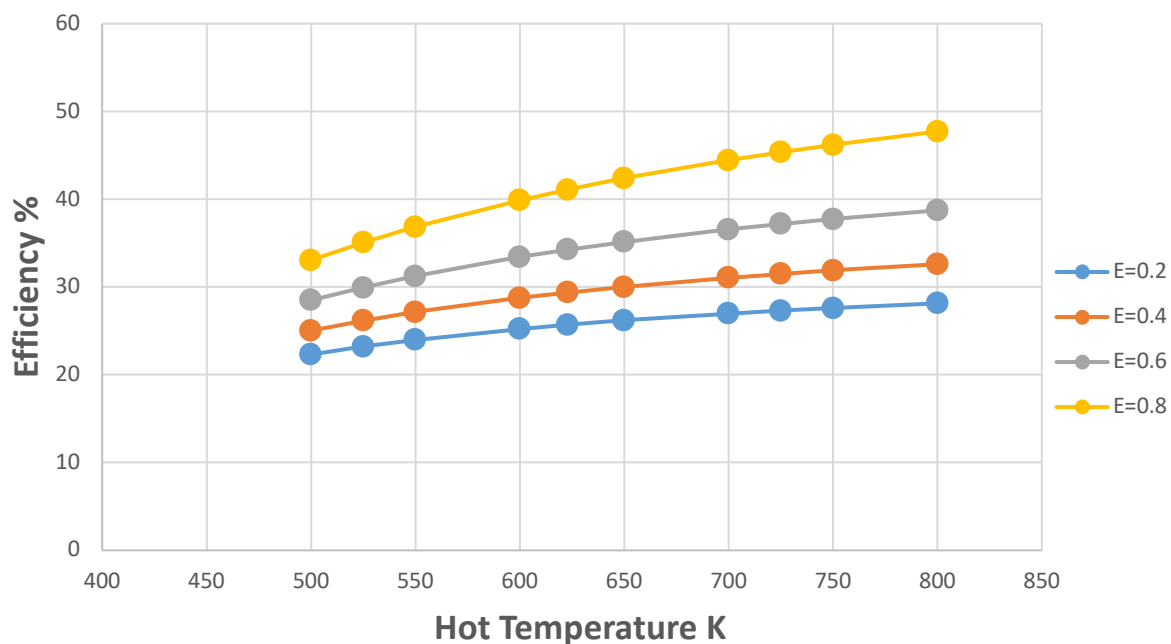


Figure 38 The variations of efficiency against hot temperature for regenerator effectiveness

3.5. Effects of cold temperature of different gasses

Increases in cold temperatures have the opposite effects on total input heat, net work, and thermal efficiency as those experienced by increases in hot temperatures. The reduction in net work will be undesirable even when a rise in cold temperature will lead to a decrease in the total input heat. Figure 39 and Figure 41 show the fluctuations of total input heat and net work

against cold temperature. Thermal efficiency drops with a rise in low temperature because the decrease in net effort is greater than the decrease in the total amount of input heat.

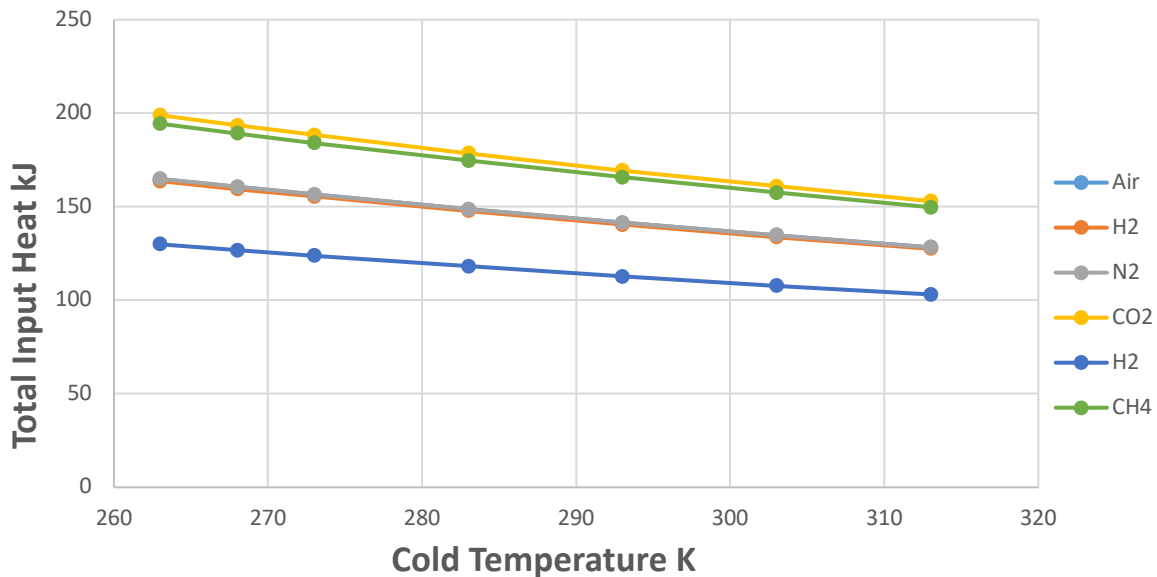


Figure 39 The variations of total input heat against cold temperature for different gasses

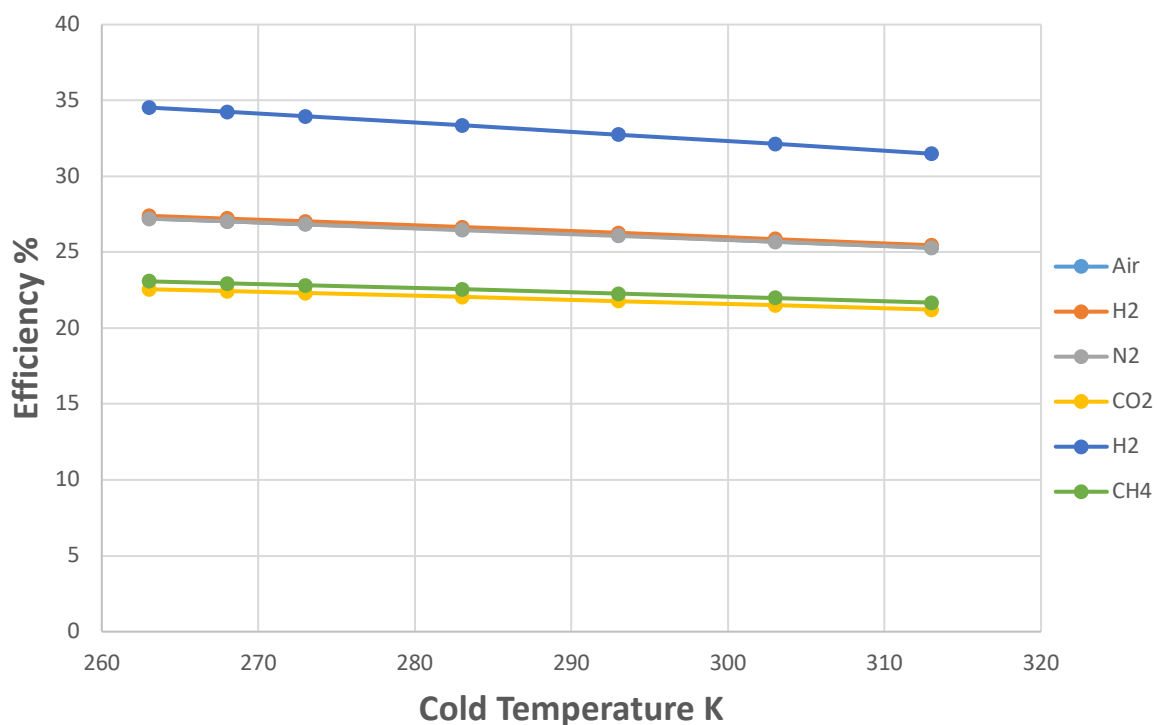


Figure 40 The variations of efficiency against cold temperature for different gasses

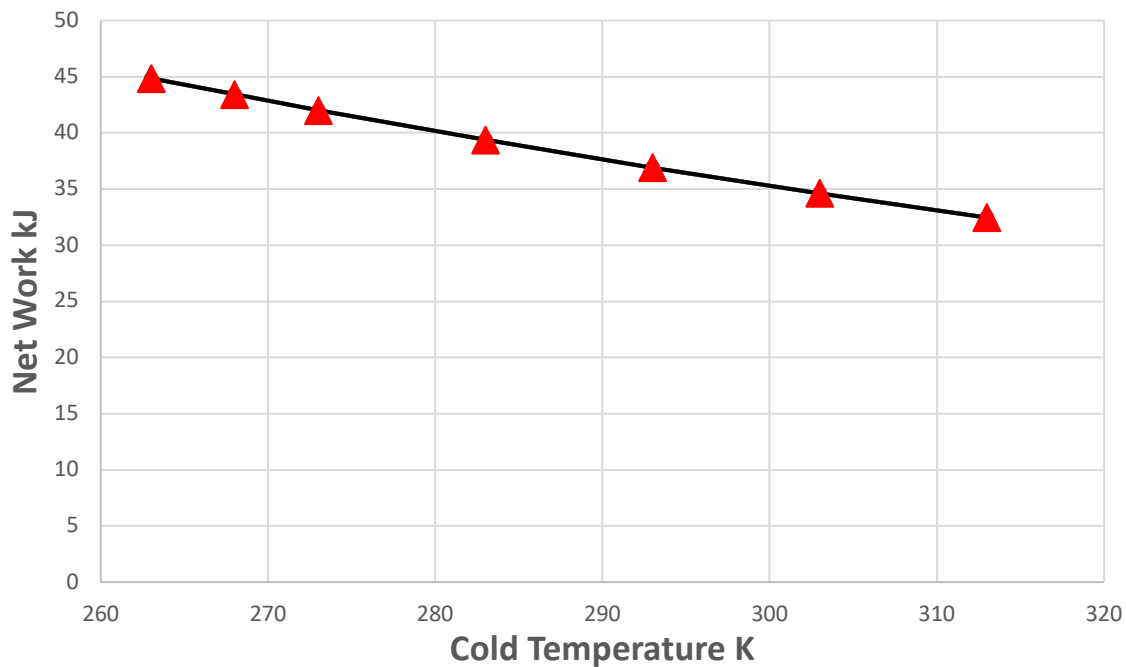


Figure 41 The variations of net work against cold temperature

3.6. The effects of regenerator effectiveness with cold temperature variations

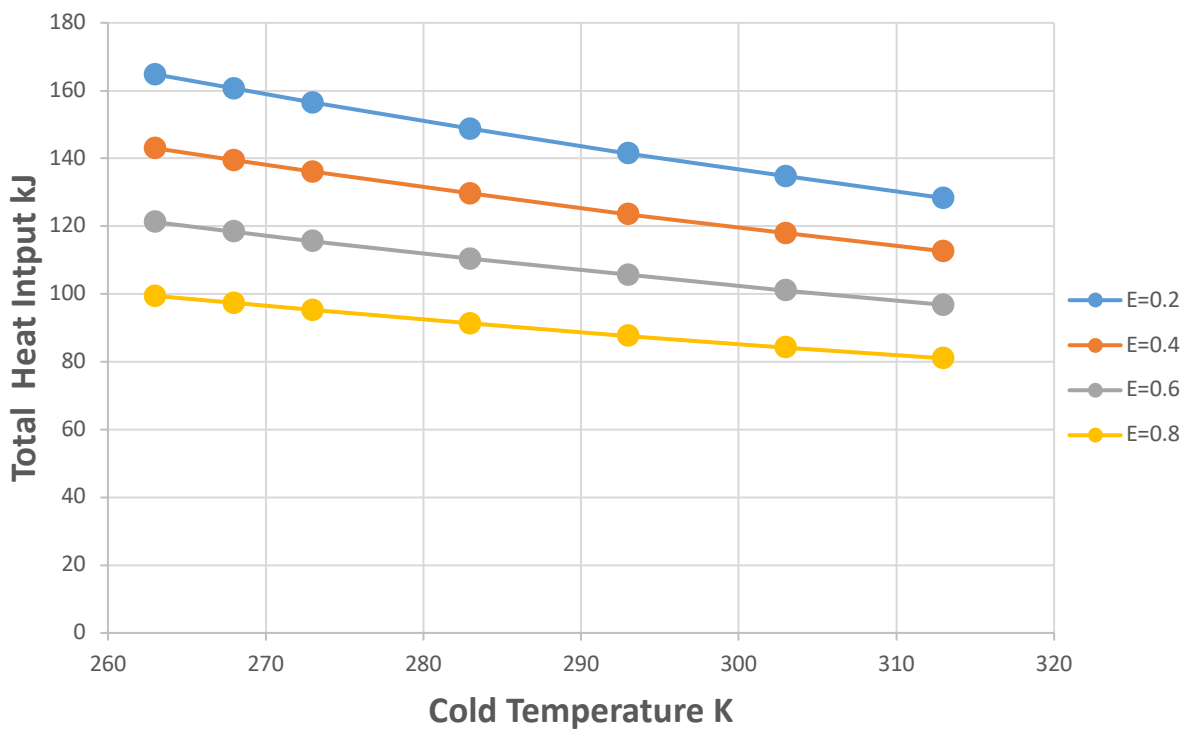


Figure 42 The variations of total input heat against cold temperature for regenerator effectiveness

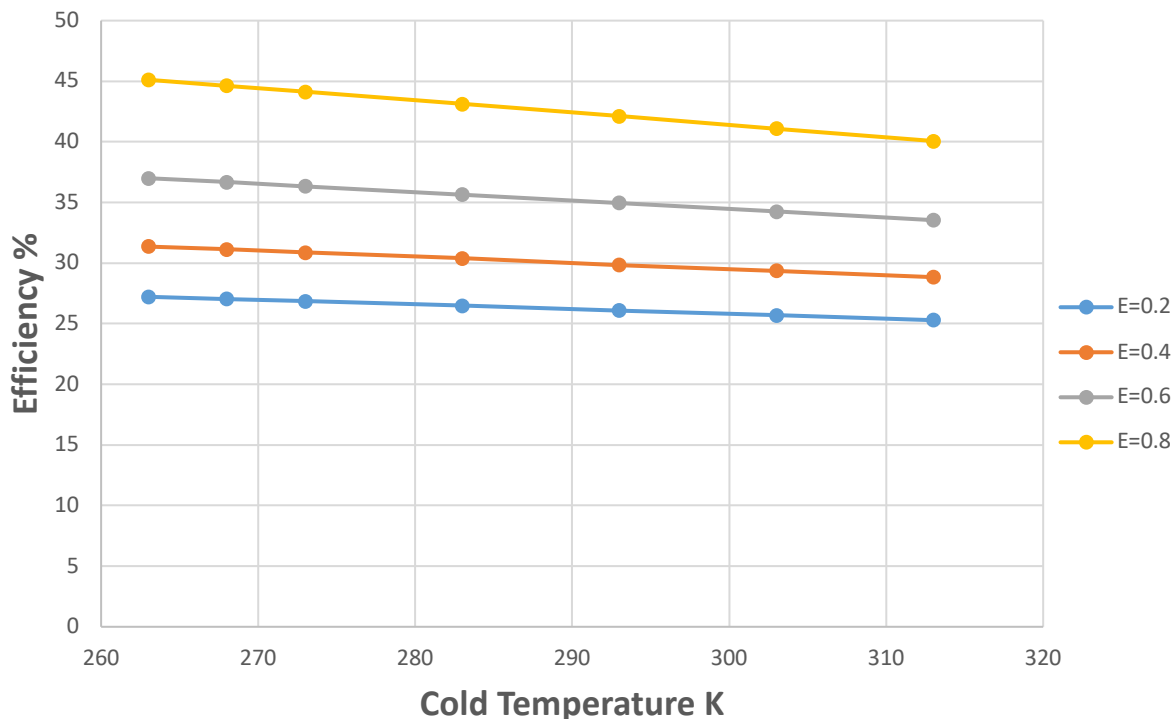


Figure 43 The variations of efficiency against cold temperature for regenerator effectiveness

3.7. The effects of regenerator effectiveness

The efficiency of the regenerator shows how much heat is needed during step 2-3 of Figure 24. Thus, having a regenerator with greater effectiveness will result in less heat input overall. Variations in total input heat against regenerator effectiveness for various working fluids are shown in Figure 44. As demonstrated, the effectiveness of regenerators has a greater impact on air, hydrogen, and nitrogen than helium. For instance, the total heat input of hydrogen falls from 160 kJ to roughly 95 kJ, or by about 59 percent.

It should be remembered that even in these circumstances, helium has a far higher thermal efficiency than other gases that are thought of as working gases. As shown in Figure 45. The thermal efficiency of all working gases reaches a constant value due to a rise in regenerator effectiveness.

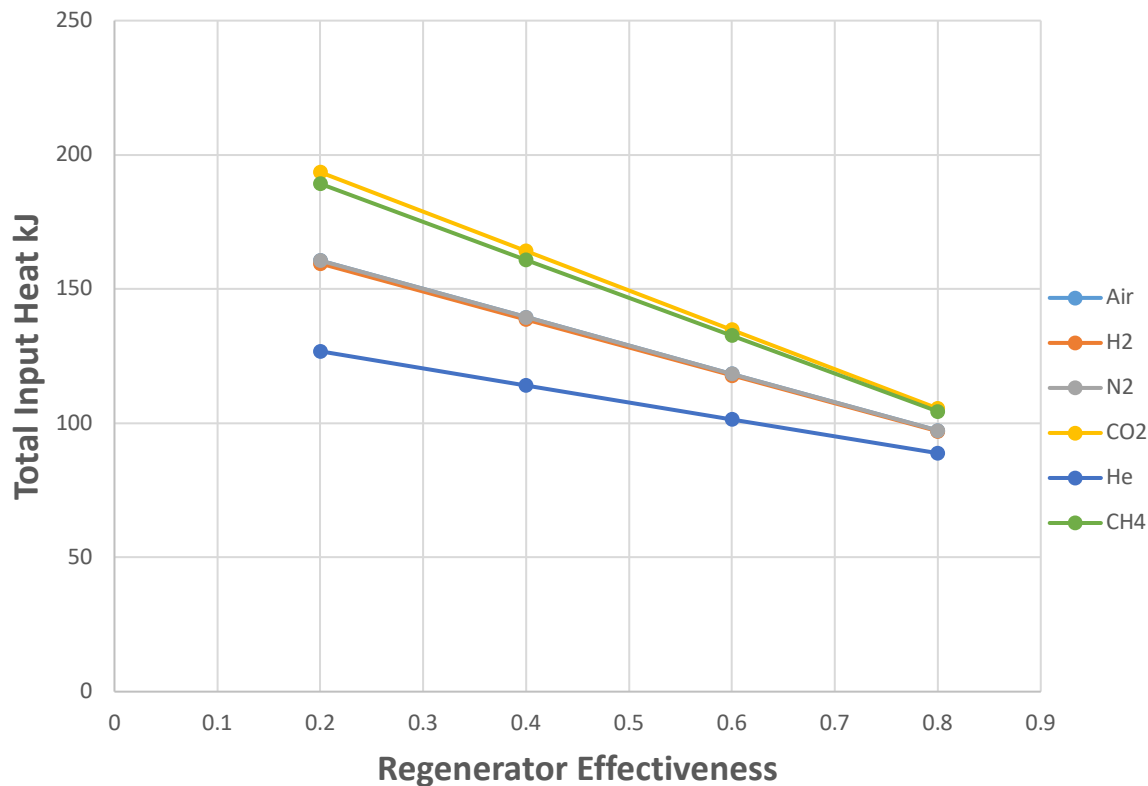


Figure 44 The variations of total input heat against regenerator effectiveness with different gasses

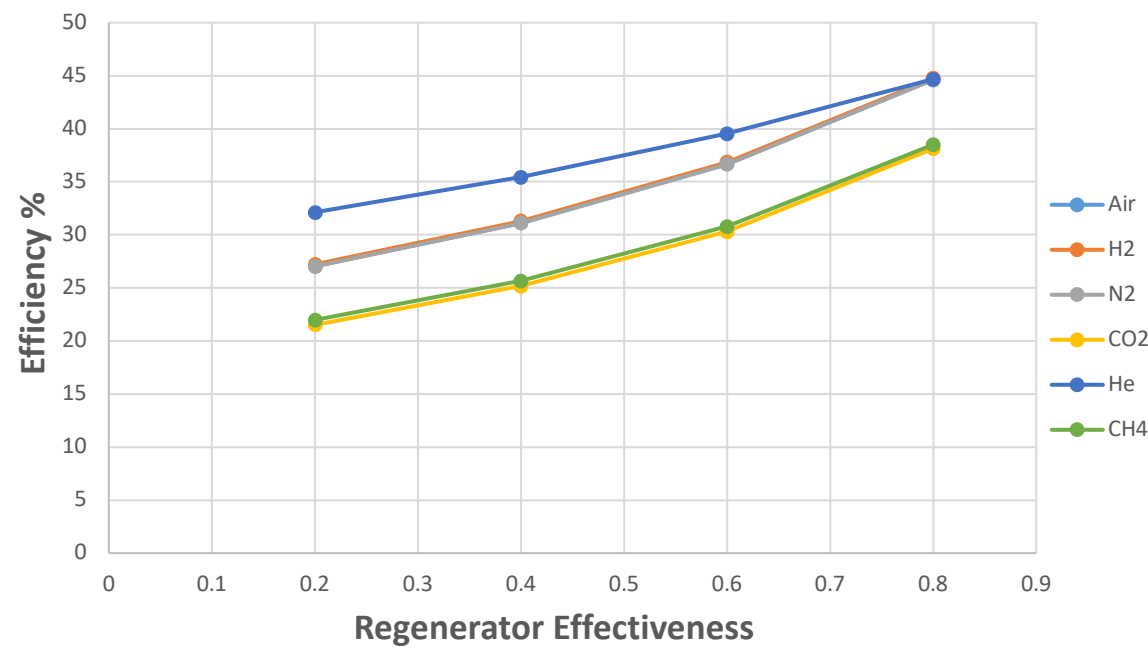


Figure 45 The variations of efficiency against regenerator effectiveness with different gasses

3.8. The effects of compression ratio of different gasses

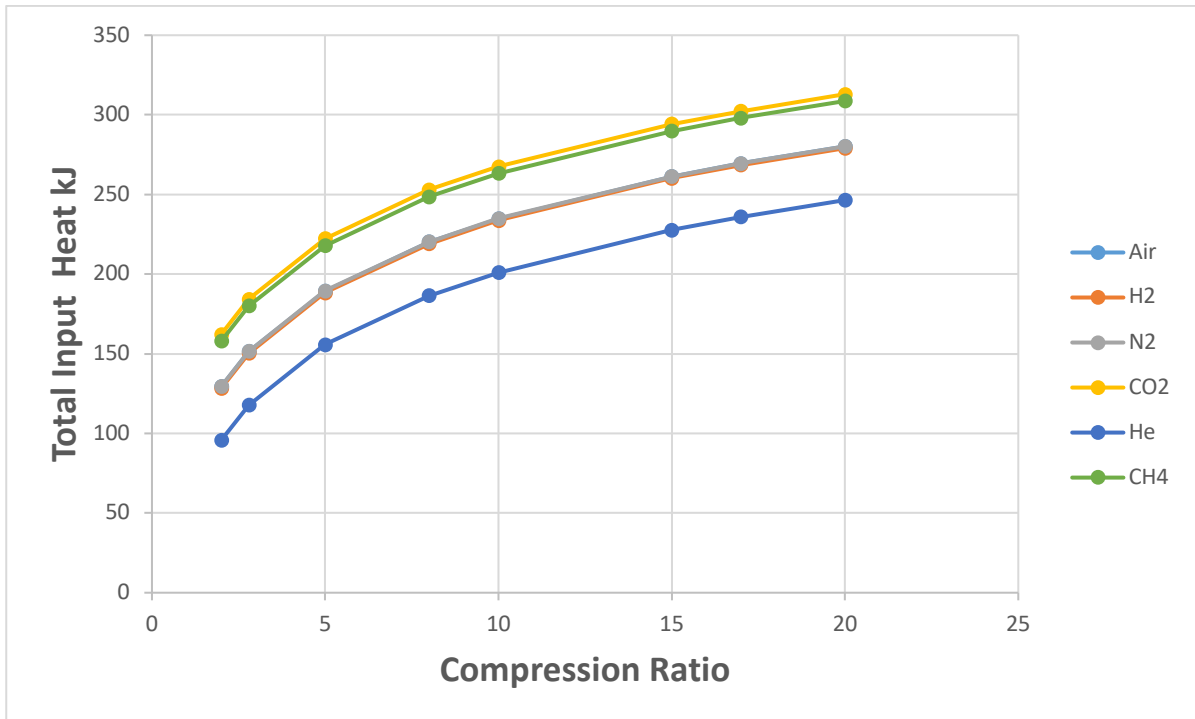


Figure 46 The variations of total input heat against compression ratio for different gasses

3.9. Effects of solar radiation on Stirling cycle

The solar radiation which is supplied to the system at the state 3-4 varies according to the each month of the year. The radiation depends on different parameters such as latitude angle, declination of the location, hour angle and solar constant which is 1367 W/m^2 . So, extraterrestrial solar radiation which is not subjected to atmosphere loss effects reaches its maximum value of $71.2 \text{ MJ/m}^2\text{-day}$ in June while its lowest is in December with the value of approximately $11.7 \text{ MJ/m}^2\text{-day}$, shown in Figure 47.

Also, it is observed that the terrestrial solar radiation which is exposed to atmosphere effects in terms of losses reaches its top point in June with $40.8 \text{ MJ/m}^2\text{-day}$. In the simulation application, month of the year can be selected to see the solar radiation on that specific time. In January, it hits the lowest point of $4.34 \text{ MJ/m}^2\text{-day}$, shown in the Figure 48.

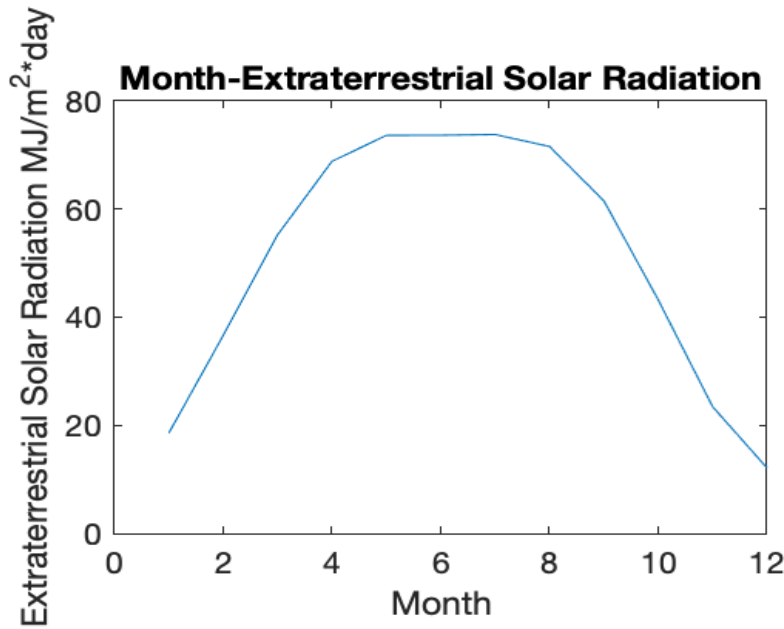


Figure 47 The variations of extraterrestrial solar radiation against month

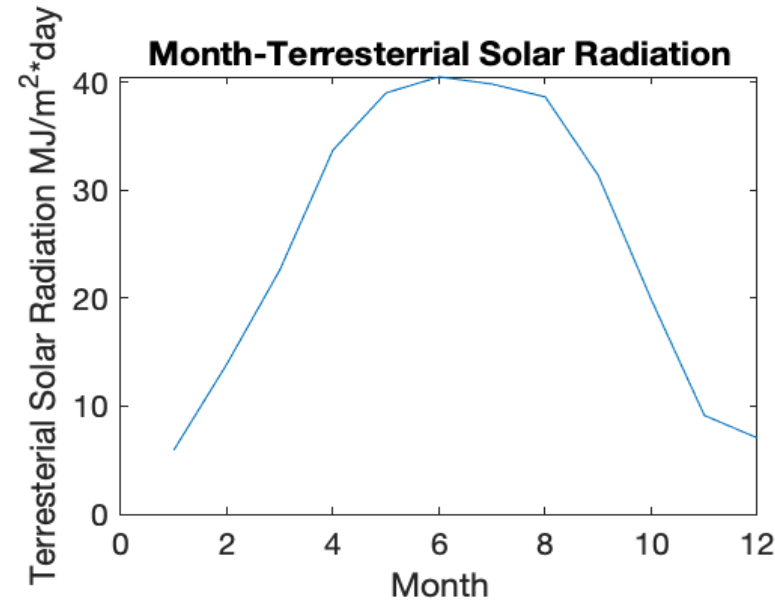


Figure 48 The variations of terrestrial solar radiation against month

3.10. Photovoltaic Panel Requirements

At the process 3-4, the system requires obvious amount of heat to keep running the cycle without fluctuations. In this study, solar energy is as an external heat source which is a heat supplier to the system. According to the isothermal expansion process, due to increase in volume, heat must be applied to the system which is equal to the extraterrestrial or terrestrial solar radiation. When the radiation is founded per meter squared, the area of photovoltaic panel

can be determined with the following equations below.

$$Q_{3-4} = I_{exterrestrial} * \text{Area of PV panel} \quad (53)$$

$$Q_{3-4} = I_{terrestrial} * \text{Area of PV panel} \quad (54)$$

The variation of hot temperature in the Figure 49 has effects on panel area. For CO₂, panel area reaches the maximum value compared to the other gasses. It reaches approximately 60 cm² at 800 K while helium reaches slight below 40 cm². Also, due to the changes in compression ratio, panel area illustrates an exponential growth while the compression ratio rises. After compression ratio of 10, panel area starts to grow linearly.

Also, compression ratio has effect on panel area, shown in Figure 50. As compression ratio increases panel area also increases with all gasses. It is observed that Helium keeps the lowest panel area values with minimum 21 cm² and maximum 60 cm².

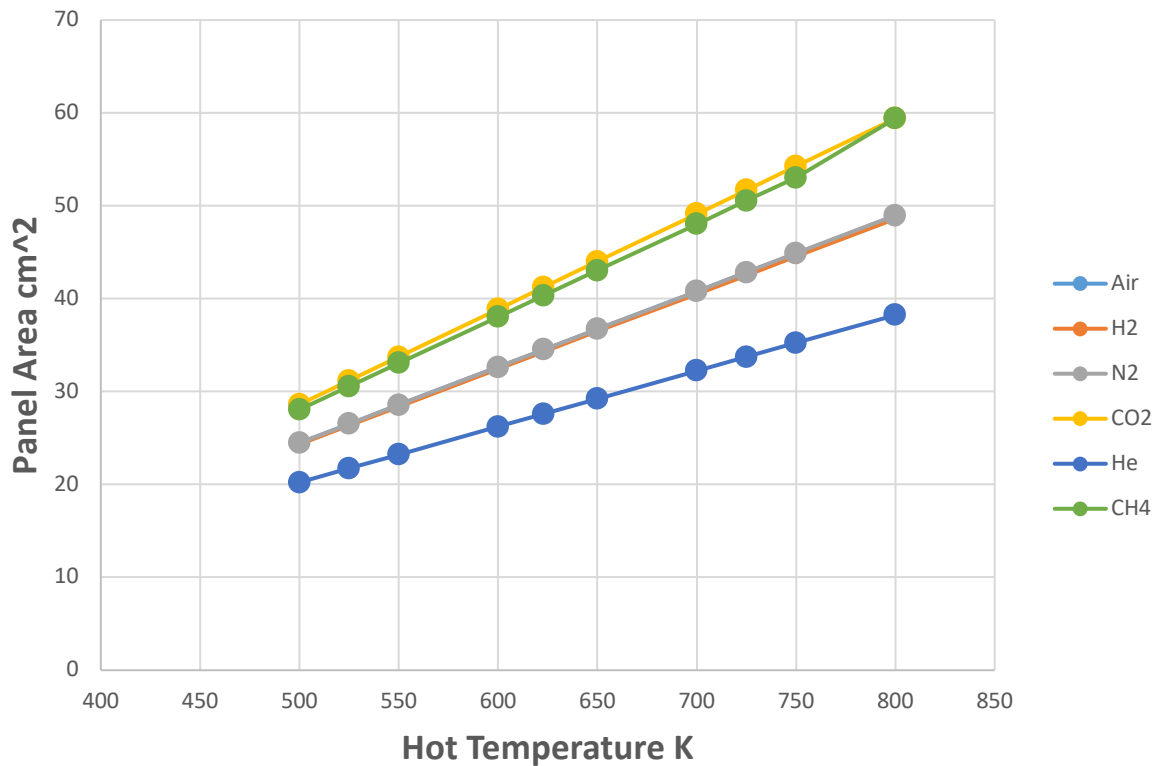


Figure 49 The variation of panel area against hot temperature of different gasses

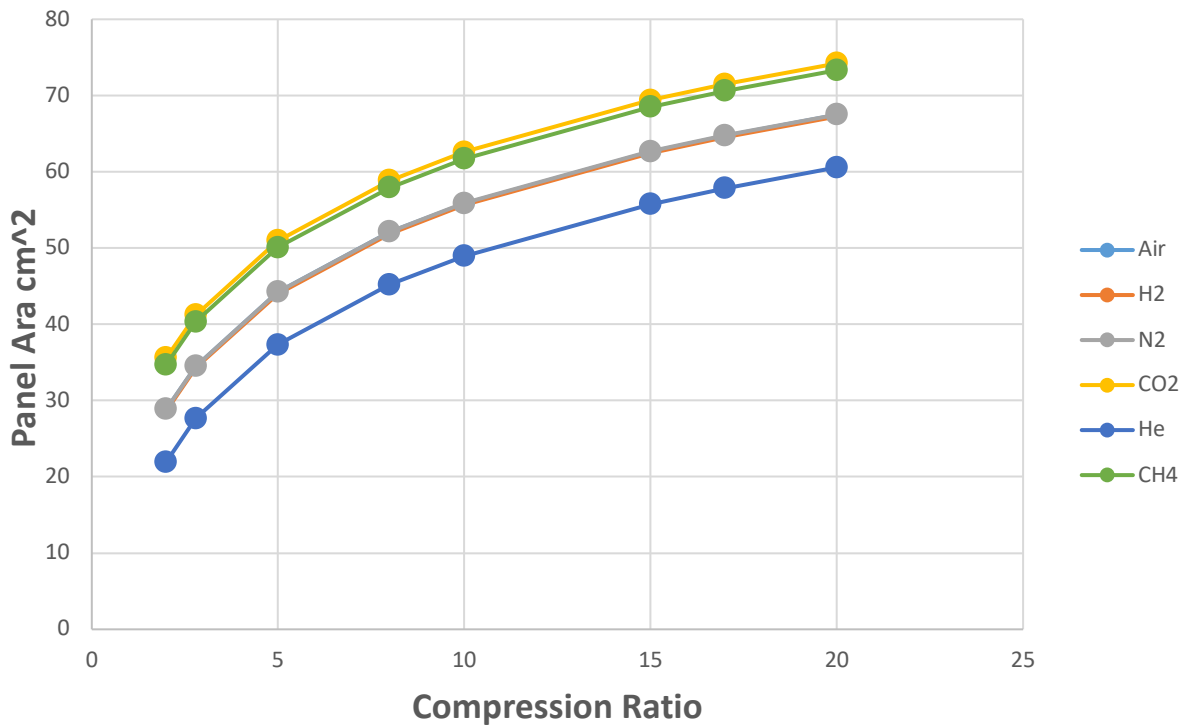


Figure 50 The variation of panel area against compression ratio of different gasses

4. CONCLUSION

In 1816, the Scottish clergyman Robert Stirling invented the Stirling engine. Since then, many research studies have been carried out on these engines, which function using a closed regenerative cycle. However, these studies have been overshadowed by the prominence of internal combustion engines.

There are several configurations of Stirling engine such as alpha, beta, gamma and free piston configurations. Their geometries and working principles differ from each other. The suitable one must be chosen for the purpose of the usage area. For instance, alpha configuration has an angle between the pistons which varies between 32 degree and 46 degree. Beta configuration works with one cylinder and two piston concentrically in the same cylinder, while, however, gamma configuration has another cylinder for the working piston.

This article performs a thorough parametric investigation on Solar Stirling Engine. Variable parameters include hot temperature, cold temperature, regenerator efficiency, working gas values. In addition to the effects of each parameter, their interactions are also discussed.

The heater's output temperature will rise, increasing both its thermal efficiency and total heat input. While the thermal efficiency results in a restricted value, the overall input heat is increased linearly. In engines with greater regenerator effectiveness, the rate of rise is significantly higher.

Thermodynamic efficiency and total input heat will increase with a decrease in colder temperature. Total input heat is raised exponentially, in contrast to fluctuations in heater temperature. Engines with better regenerator efficacy experience a significantly slower rate of overall input heat growth.

Engines with more effective regenerators use less heat overall, which results in improved thermal efficiency.

The way of calculation of solar radiation, there are several parameters such as declination angle, latitude, hour angle, azimuth angle, zenith angle and elevation. These parameters are related to the location and time due to the movements of the sun. After these variables are calculated, extraterrestrial which is not affected by atmosphere (atmosphere effects are neglected) or terrestrial solar radiation which has atmospherically losses can be calculated.

Photovoltaic solar panels have different types in terms of the solar cell types such as monocrystalline, polycrystalline and amorphous (thin-film). Due to the differences of solar panels, their efficiencies vary with the solar cell type. Their efficiencies occur in the range of 12% and 25%. For the design, the most appropriate one must be chosen to reach design considerations. The solar radiations projected on the solar panels and the panel convert them into electrical energy which supplies heating in device.

In this study, it is investigated that how the analysis of thermodynamic processes is done. Working principles of solar panels and their usage purposes have been determined. The variations of solar radiation with different variables are analyzed. With these analysis, calculations are made and several graphs of different parameters are investigated. According to the graphs, the outcomes are considered in the perspective of engineering.

5. REFERENCES

- [1] Wilson, Alex (April 29, 2010). "Building Green's Product of the Week". Stirling SunCatcher with "Heat Engine" Technology. Building Green.com. Archived from the original on July 8, 2011. Retrieved 2011-03-03.
- [2] What is Microgeneration? And what is the most cost effective in terms of CO2 reduction". Claverton-energy.com. 2008-11-06. Retrieved 2009-07-24.
- [3] Hasci, James (14 July 2008). "Modified Stirling Engine With Greater Power Density". Create the Future Design Contest. National Aeronautics and Space Administration & SolidWorks.
- [4] "Science: A Stirling Performance". Time. 9 September 1974. Archived from the original on June 14, 2008.
- [5] Nightingale, Noel P. (October 1986). "Automotive Stirling Engine Mod II Design Report" (PDF). National Aeronautics and Space Administration and U.S. Department of Energy.
- [6] Mcconaghy, Robert (1986). "Design of a Stirling Engine for Model Aircraft".
- [7] A review of Stirling-engine-based combined heat and power technology Shunmin Zhu Guoyao Yu , Kun Liang , Wei Dai Ercang Luo
- [8] Performance analysis of different working gases for concentrated solar gas engines: Stirling & Brayton Mohamed A. Sharaf Eldean*, Khwaja M. Rafi A.M. Soliman
- [9] Poullikkas A, Kourtis G, Hadjipaschalis I. Parametric analysis for the installation of solar dish technologies in Mediterranean regions. Renew. Sustain. Energy Rev. 2010;14(9):2772– 83.
- [10] Ranieri, Salvatore & Prado, Gilberto & Macdonald, Brendan. (2018). Efficiency Reduction in Stirling Engines Resulting from Sinusoidal Motion. Energies. 11. 2887. 10.3390/en11112887.
- [11] Shufat, S, Kurt, E, Elhadad, K, Hancerliogullari, A. A Numerical model for a Stirling engine, Journal of Energy Systems 2018; 2(1), 1-12, DOI: 10.30521/jes.379164
- [12] Lujean Ahmad, Navid Khordehgah, Jurgita Malinauskaite, Hussam Jouhara, Recent advances and applications of solar photovoltaics and thermal technologies,Energy,Volume 207,2020,118254,ISSN 0360-5442,<https://doi.org/10.1016/j.energy.2020.118254>.
- [13] Ullal HS. Overview and challenges of thin film solar electric technologies overview and challenges of thin film solar electric technologies. World Renew Energy Congr X Exhib 2008:1e4

- [14] Chen F, Wang L. Light trapping design in silicon-based solar cells. *Sol Cells - Silicon Wafer-Based Technol* 2012;255e74.
- [15] Nyarko Kumi Ebenezer, Brew-Hammond Abeeku. Design and analysis of a 1MW grid-connected solar PV system in Ghana. *African Technol Policy Stud Netw* 2013. <https://doi.org/10.1162/itgg.2009.4.4.301>.
- [16] Tripathy M, Sadhu PK, Panda SK. A critical review on building integrated photovoltaic products and their applications. *Renew Sustain Energy Rev* 2016;61:451e65. <https://doi.org/10.1016/j.rser.2016.04.008>.
- [17] Nogueira CEC, Bedin J, Niedzialkoski RK, de Souza SNM, das Neves JCM. Performance of monocrystalline and polycrystalline solar panels in a water pumping system in Brazil. *Renew Sustain Energy Rev* 2015;51:1610e6. <https://doi.org/10.1016/J.RSER.2015.07.082>.
- [18] Peng Z, Herfatmanesh MR, Liu Y. Cooled solar PV panels for output energy efficiency optimisation. *Energy Convers Manag* 2017;150:949e55. <https://doi.org/10.1016/J.ENCONMAN.2017.07.007>.
- [19] Fraunhofer. New world record for solar cell efficiency at 46% e French- German cooperation confirms competitive advantage of European photo- voltaic industry 2019. <https://www.ise.fraunhofer.de/en/press-media/press-releases/2014/new-world-record-for-solar-cell-efficiency-at-46-percent.html>.
- [20] Eddie W.K. WU IPLL. The potential application of amorphous silicon photo- voltaic technology in Hong Kong. n.d.
- [21] Wang Yang, Sun Tianyi, Paudel Trilochan, Zhang Yi, Ren Zhifeng, Kempa K. Metamaterial-plasmonic absorber structure for high efficiency amorphous silicon solar cells. *Nano Lett* 2012;12:440e5.
- [22] Alazzawi, Shurooq & Al-Hilaly, Emad. (2018). Sum-Sines Equation For Estimating The Percent Of Shadow Length Of Targets In The Satellite Images.
- [23] P. I. Cooper, “The absorption of radiation in solar stills”, *Solar Energy*, vol. 12, pp. 333 - 346, 1969.
- [24] Md. Shariful Alam Emon, Mohsan Uddin Ahmad, Md Hasanuzzaman, Chapter 2 - Solar thermal energy conversion, Technologies for Solar Thermal Energy, Academic Press, 2022, Pages 25-54, ISBN 9780128239599, <https://doi.org/10.1016/B978-0-12-823959-9.00011-8>.
- [25] Sherihan Abd El-Ghafour, Nady Mikhael, Mohamed El-Ghandour, Design and Three-Dimensional Simulation of a Solar Dish-Stirling Engine, *Mechanical Power Engineering*

Department, Faculty of Engineering, Port-Said University, Egypt.
<https://doi.org/10.37934/arfmts.82.1.5176>

- [26] Jigui Zheng, Jing Chen, Ping Zheng, Hongxing Wu, Chengde Tong, Research on Control Strategy of Free-Piston Stirling Power Generating System, Energies 2017, 10(10), 1609; School of Electrical Engineering and Automation, Harbin Institute of Technology, Harbin 150080, China <https://doi.org/10.3390/en10101609>
- [27] Asnaghi, Abolfazl & Lajevardi, S.M & Saleh Izadkhast, Pejman & Haghparast Kashani, Arash. (2012). Thermodynamics Performance Analysis of Solar Stirling Engines. ISRN Renewable Energy. 2012. 10.5402/2012/321923.
- [28] Luo, Zhongyang & Sultan, Umair & Ni, Mingjiang & Peng, Hao & Bingwei, Shi & Xiao, Gang. (2016). 201608 Multi-objective optimization for GPU3 Stirling engine.
- [29] Martins, Otaniel & Fernande, Erllon & Teixeira, Arleson & dos Santos Atherly Pedraça, Aline & Pedraça, João & LIMA, AMARILDO & JUAN, JOSÉ. (2021). Closed Cycle Thermal Engine: One Comparative Study for Battery Supply of Mobile Phones. European Academic Research. VIII. 6030.
- [30] Zhang, Yichao & Wijeratne, Lakitha & Talebi, Shawhin & Lary, David. (2021). Machine Learning for Light Sensor Calibration. Sensors. 21. 6259. 10.3390/s21186259.
- [31] Alazzawi, Shurooq & Al-Hilaly, Emad. (2018). Sum-Sines Equation For Estimating The Percent Of Shadow Length Of Targets In The Satellite Images.
- [32] Menniti, Daniele & Sorrentino, Nicola & Pinnarelli, A. & Burgio, Alessandro & Brusco, G. & Belli, Grazia. (2014). The concentrated solar power system with Stirling technology in a micro-grid: The simulation model. 2014 International Symposium on Power Electronics, Electrical Drives, Automation and Motion, SPEEDAM 2014. 253-260. 10.1109/SPEEDAM.2014.6872095.
- [33] Aksoy, F. Solar Energy Application Stirling Engine, Gazi University, 2011.
- [34] Sendy A. Pros and cons of monocrystalline vs polycrystalline solar panels. Solar Rev 2019. <https://www.solarreviews.com/blog/pros-and-cons-of-monocrystalline-vs-polycrystalline-solar-panels>. [Accessed 20 April 2019].
- [35] Saga T. Advances in crystalline silicon solar cell technology for industrial mass production. NPG Asia Mater 2010;2:96e102. <https://doi.org/10.1038/asiamat.2010.82>.
- [36] Pillai U. Drivers of cost reduction in solar photovoltaics. Energy Econ 2015;50:286e93. <https://doi.org/10.1016/j.eneco.2015.05.015>
- [37] Kang H, Hong T, Lee M. Technical performance analysis of the smart solar photovoltaic blinds based on the solar tracking methods considering the climate factors. Energy Build

2019;190:34e48. <https://doi.org/10.1016/j.enbuild.2019.02.013>.

[38] Shukla AK, Sudhakar K, Baredar P. Recent advancement in BIPV product technologies: a review. *Energy Build* 2017;140:188e95. <https://doi.org/10.1016/j.enbuild.2017.02.015>.

[39] Febba DM, Rubinger RM, Oliveira AF, Bortoni EC. Impacts of temperature and irradiance on polycrystalline silicon solar cells parameters. *Sol Energy* 2018;174:628e39. <https://doi.org/10.1016/j.solener.2018.09.051>.

[40] Day J, Senthilarasu S, Mallick TK. Improving spectral modification for applications in solar cells:a review.*Renew Energy* 2019;132:186e205.

<https://doi.org/10.1016/j.renene.2018.07.101>.

[41] Lee TD, Ebong AU. A review of thin film solar cell technologies and chal- lenges. *Renew Sustain Energy Rev* 2017;70:1286e97. <https://doi.org/10.1016/j.rser.2016.12.028>.

[42] Efficiency Analysis Of The Effect Of Radiation And Temperature On Photovoltaic Monocrystalline, Polycrystalline, And Amorphous Recorded By Data Logger Based On Arduino Mega 2560 Armin Sofijan1, Bhakti Y. Suprapto2, Zainuddin Nawawi Department of Electrical Engineering, Engineering Faculty, Sriwijaya University, Indonesia

[43] Panasonic. Amorton - amorphous silicon solar cells 2018. <https://www.panasonic-electric-works.com/eu/amorton-amorphous-silicon-solar-cells.htm> (accessed April 25, 2019).

[44] Ali Binbir, Değişken Faz Açılı Alfa Tipi Bir Stirling Motorunun İmalati Ve Testleri, Afyon Kocatepe Üniversitesi, Fen Bilimleri Enstitüsü. Temmuz 2017

[45] T. Kodama, High-temperature solar chemistry for converting solar heat to chemical fuels, *Progress in Energy and Combustion Science*, Volume 29, Issue 6, 2003, Pages 567-597, ISSN 0360-1285, [https://doi.org/10.1016/S0360-1285\(03\)00059-5](https://doi.org/10.1016/S0360-1285(03)00059-5).

[46] Singh, Uday Raj & Kumar, Anil. (2018). Review on Solar Stirling Engine: Development and Performance. *Thermal Science and Engineering Progress*. 8. 10.1016/j.tsep.2018.08.016.

[47] Crandall R, Luft W. The future of amorphous silicon photovoltaic technology. 1995